Palaeogeography, Palaeoclimatology, Palaeoecology 490 (2018) 415–430

Contents lists available at ScienceDirect

Palaeogeography, Palaeoclimatology, Palaeoecology

journal homepage: www.elsevier.com/locate/palaeo

Evidence of early C_4 grasses, habitat heterogeneity, and faunal response during the Miocene Climatic Optimum in the Mojave Region

Tara M. Smiley[a,*], Ethan G. Hyland[a,b], Jennifer M. Cotton[a,c], Robert E. Reynolds[d]

[a] Department of Earth and Environmental Sciences, University of Michigan, Ann Arbor, MI 48109, United States
[b] Department of Earth and Space Sciences, University of Washington, Seattle, WA 98195, United States
[c] Department of Geological Sciences, California State University Northridge, Northridge, CA 91330, United States
[d] Desert Symposium (www.Desertsymposium.org), Redlands, CA 92373, United States

ARTICLE INFO

Keywords:
Crowder Formation
Cajon Valley Formation
Mammal diversity
Stable isotopes
Phytolith assemblages
Paleoprecipitation

ABSTRACT

Major changes to landscapes, climate, and mammalian faunas occurred at the regional scale in western North America during the Miocene Climatic Optimum (MCO) between ~17 and 14 Ma, but few studies have looked at how the MCO affected basin-scale environments. Paleoenvironmental reconstructions coupled with mammalian fossil assemblages from the Crowder and Cajon Valley formations in the Mojave Desert, California, contribute insights into local-scale (10s of kilometers) responses to warming during the Hemingfordian and Barstovian North American Land Mammal Ages. By integrating lithological descriptions, phytolith analyses, carbon isotope composition of preserved soil organic matter ($\delta^{13}C_{SOM}$), and elemental geochemistry of paleosols, we provide reconstructions of depositional environments, vegetation, and precipitation through the MCO. Phytolith and $\delta^{13}C_{SOM}$ evidence suggest that paleoenvironments were predominately C_3 grasslands, with the earliest potential presence of C_4 grasses in the region found within the Crowder Formation at ~17 Ma. Based on elemental geochemistry of paleosols, mean annual precipitation estimates are 807 (± 182) mm yr^{-1} at 17 Ma in the Crowder Formation and 740–800 (± 182) mm yr^{-1} from 16 to 15 Ma in the Cajon Valley Formation. Our multiproxy approach indicates that the Crowder and Cajon Valley basins were stable, large-scale braided stream and floodplain systems with intermittent paleosol development and heterogeneity in vegetation and moisture conditions across spatial scales. Overall, we find a signal of local paleoenvironmental stability during the MCO; however, a significant drying trend in the Crowder Formation does correspond with faunal turnover and reduction in the number of taxa present. High species diversity within faunal assemblages, especially among small mammals, and fewer shared species between the Crowder and Cajon Valley assemblages than expected based on bootstrap analysis indicate that peak mammal diversity was accommodated at both local and regional scales during sustained tectonic activity and the MCO in western North America.

1. Introduction

1.1. Miocene Climatic Optimum and mammal diversity

The middle Miocene was an important period of climate and landscape change that reshaped biotas and environments over local to global scales (e.g., Janis et al., 2000; Tedford et al., 2004; Riddle et al., 2014; Samuels and Hopkins, 2017). Key events during this interval included increased global temperatures during the Miocene Climatic Optimum (MCO; peak warming ~17–14.75 Ma) followed by persistent cooling through the remainder of the Neogene (Zachos et al., 2001; Goldner et al., 2014), a gradual transition from forested ecosystems to grasslands in the Great Plains and western North America (e.g., Strömberg, 2005; Edwards et al., 2010; Strömberg and McInerney, 2011; Harris et al., 2017), and the formation of the topographic complexity in the Basin and Range province (e.g., Dickinson, 2006). From the early Miocene (~23 Ma) to the present, tectonic extension west of the Rocky Mountains increased overall habitat area by ~400,000 km^2, steepened environmental gradients, and generated a topographic fabric of alternating isolated basins and mountain ranges (McQuarrie and Wernicke, 2005). Interactions between tectonic forces, climate warming, and vegetation change produced a landscape of high relief and habitat heterogeneity with significant consequences for mammalian diversity, evolution, and biogeography. At the regional scale, peak mammal diversity and taxonomic turnover in the fossil record of western North America have often been linked to the MCO and

* Corresponding author.
E-mail address: smileyta@oregonstate.edu (T.M. Smiley).

https://doi.org/10.1016/j.palaeo.2017.11.020
Received 5 June 2017; Received in revised form 3 November 2017; Accepted 7 November 2017
Available online 11 November 2017

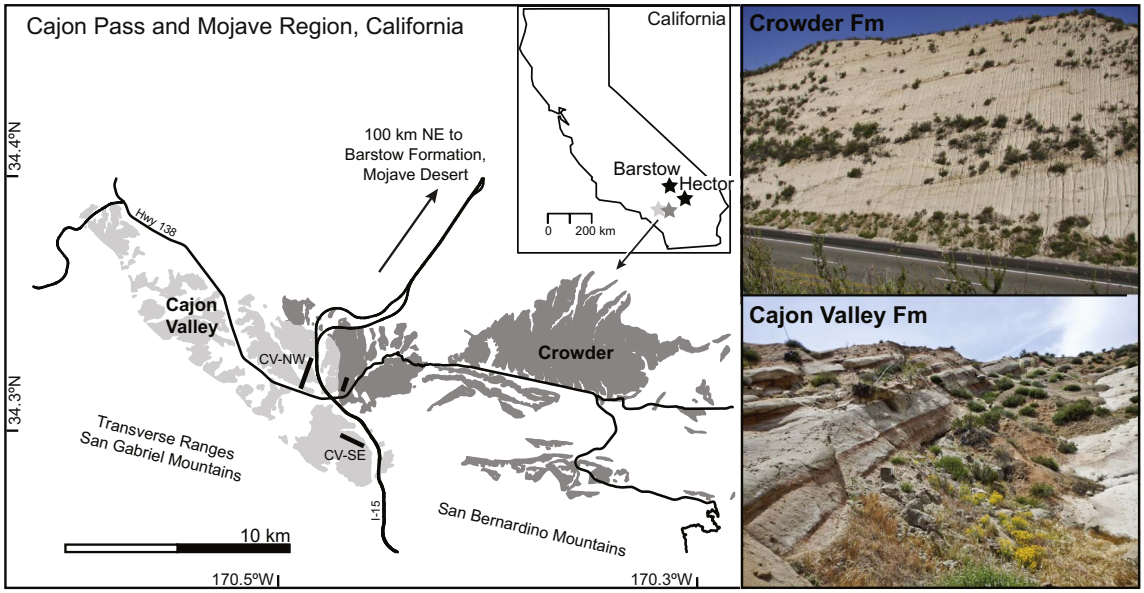

Fig. 1. Geographic location of the study area and field photos of paleosol units within the Crowder Formation (dark gray) and Cajon Valley Formation (light gray). Thick black bars indicate the position of the measured sections presented in this study. Map inset shows location of the middle Miocene formations in Cajon Pass and the Mojave Desert, including Crowder, Cajon Valley, Hector, and Barstow formations. (For interpretation of the references to color in this figure legend, the reader is referred to the web version of this article.) Geologic map data are from Morton and Miller (2006).

intensification of tectonic activity from 18 to 14 Ma (Barnosky and Carrasco, 2002; Kohn and Fremd, 2008; Finarelli and Badgley, 2010; Badgley et al., 2014). Following the MCO, declines in species richness and the loss of low-crowned, closed-habitat taxa have been related to cooling and an increase in grassland and arid ecosystems across North America into the late Miocene (e.g., Janis et al., 2004; Figueirido et al., 2012; Samuels and Hopkins, 2017). However, coupled records of local environmental change and ecological response are sparse and the contribution of basin-scale faunas to regional diversity changes during the Miocene remains unresolved.

In order to evaluate paleoecological communities across this interval of increased tectonic activity and global temperatures, a sedimentary and fossil record that captures changes in faunal composition spanning the MCO is critical. Within North America, fossil-rich formations in the Mojave Desert and Cajon Pass regions of southern California, USA (Fig. 1) represent a rare continuous record through the MCO and fill an important geographic gap in our understanding of local environmental and faunal dynamics during this important transitional period. Together, the well-documented Barstow Formation and less well-studied Cajon Valley, Crowder, and Hector formations extend over the middle Miocene from 22.9 to 12.5 Ma and preserve a diversity of small and large mammal fossils (Lindsay, 1972; Miller, 1980; Woodburne et al., 1990; Tedford et al., 2004). In this study, we investigate the geological, paleoenvironmental, paleoclimatic, and faunal history of the Crowder and Cajon Valley formations in the vicinity of the Cajon Pass region during the MCO. These formations preserve mammalian faunas that occurred on the edge of the Basin and Range Province from the mid-Hemingfordian through the Barstovian North American Land Mammal Ages (NALMA), or approximately 17–13.7 Ma (Woodburne and Golz, 1972; Reynolds et al., 2008). The primary aims of this paper are to: 1) present a revised stratigraphic framework for the known mammalian faunal assemblages, 2) establish paleoenvironmental reconstructions of vegetation from phytolith assemblages and the carbon isotope composition of preserved soil organic matter, 3) estimate mean annual precipitation and infer variation in moisture conditions based on the elemental geochemistry and carbon isotope composition of paleosols, and 4) examine variation in taxonomic richness and composition contemporaneous with paleoenvironmental reconstructions. The integration of these records enables us to test how local ecosystems responded to global climate and regional tectonic changes. We hypothesize that long-term warming during the MCO followed by long-term cooling should drive local shifts in vegetation, aridity, and consequently faunal composition in the Crowder and Cajon Valley formations. For example, increases in aridity and the relative proportion of grass in local ecosystems may have led to decreased species richness and the loss of browser taxa, especially among rodents (e.g., Janis et al., 2004; Samuels and Hopkins, 2017). Furthermore, we hypothesize that as topographic complexity increased during this interval, notable differences in habitats and mammal assemblages (e.g., high provinciality) arose across adjacent and near-by basins. The documentation of spatial and temporal faunal turnover within the Mojave region can in turn inform the processes that generate and maintain high regional diversity across western North America during the MCO.

1.2. Age constraints

Fossil collection in the Crowder and Cajon Valley formations has occurred over the last five decades, with notable recovery of small-mammal fossils due to extensive screen-washing efforts. To date, 56 identified taxa of small (n = 33) and large (n = 23) mammals are known from the two formations (Woodburne and Golz, 1972; Reynolds, 1991; Reynolds et al., 2008). Highly fossiliferous assemblages of both large and small mammals, in addition to several dated tuffs, make the Barstow Formation of the western Mojave Desert a useful reference for biostratigraphic and chronostratigraphic correlation with the Crowder and Cajon Valley formations. Mammalian assemblages of the Crowder and Cajon Valley formations overlap biostratigraphically with those of the Barstow Formation; however, the Crowder and Cajon Valley formations also record an older Hemingfordian fauna that coincided with early MCO warming. Age determination based on biostratigraphic correlation, faunal zones from the Barstow Formation, and paleomagnetic stratigraphy indicate that the Crowder Formation was deposited between 17.5 and 7.1 Ma or younger (Reynolds et al., 2008), and the Cajon Valley Formation between 18.0 and 12.7 Ma; however, fossils do not occur throughout the entire depositional histories of these basins (Woodburne and Golz, 1972; Winston, 1985; Weldon, 1986; Liu, 1990; Reynolds et al., 2008).

Lithological variation in sediment type and depositional frequency

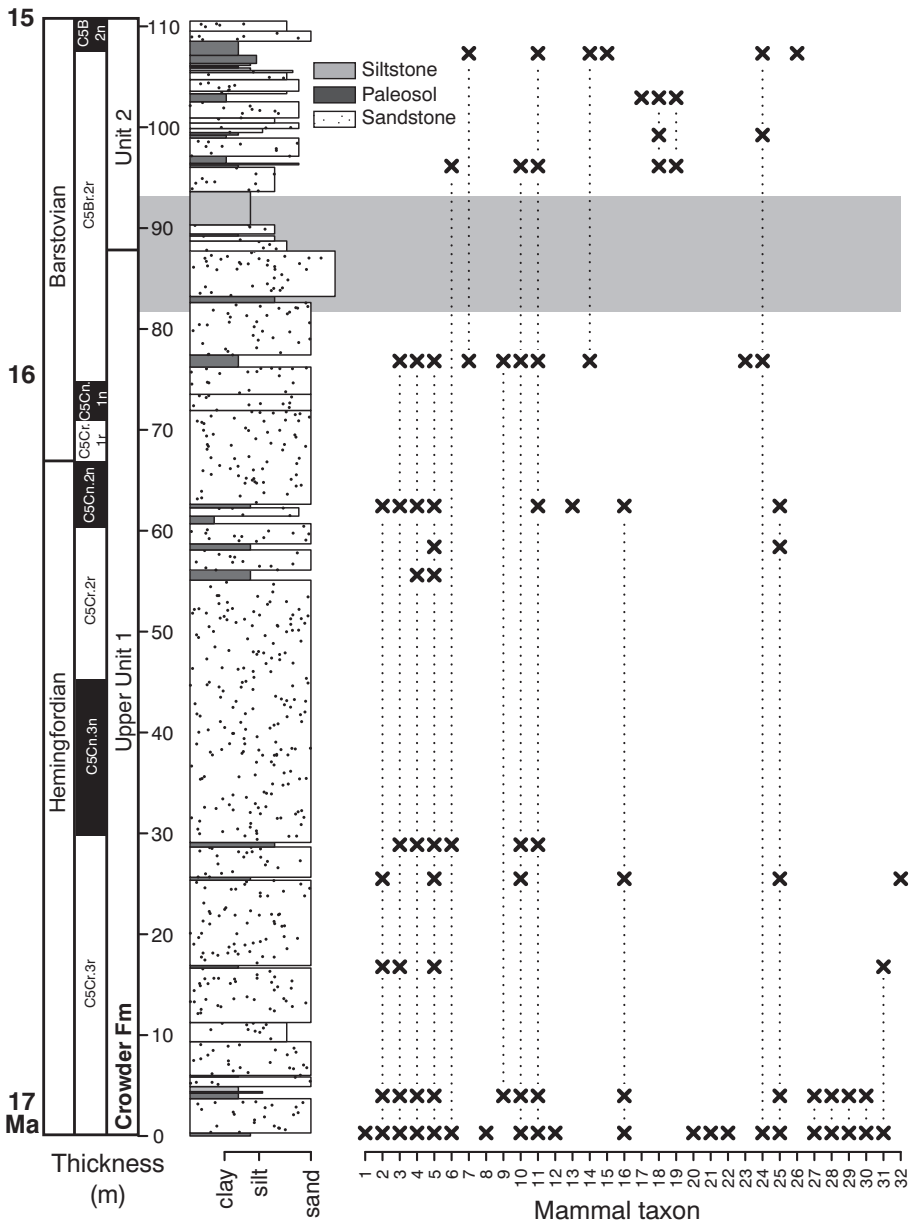

Fig. 2. Stratigraphic section for the Crowder Formation, Upper Unit 1 and Unit 2. Temporal correlation with the NALMA and global geomagnetic polarity timescales (Woodburne, 1987; Gradstein et al., 2004) is shown. Fossil occurrences of taxa listed in Table 1 are indicated by an x in relation to the stratigraphic section and biostratigraphic ranges (dotted lines) are assumed to range through the first and last occurrences of taxa within the formation. The horizontal gray bar indicates the interval of most pronounced environmental and faunal change. Ages of the sedimentary strata and fossil localities are inferred from paleomagnetic data from Winston (1985) and Weldon (1986), and biostratigraphy and paleomagnetic age interpretations from Reynolds et al. (2008).

in the Crowder and Cajon Valley formations is the basis for subdividing the strata into five and six, respectively, distinct and laterally extensive units (Woodburne and Golz, 1972; Foster, 1980). Fossils of the Hemingfordian and Barstovian NALMAs span Units 1 and 2 within the Crowder Formation and Units 3 through 5 within the Cajon Valley Formation (Figs. 2 and 3; Woodburne and Golz, 1972; Weldon, 1986). Since Hemingfordian and Barstovian strata within the Crowder and Cajon Valley formations record local environments and faunal assemblages in relation to the MCO and regional tectonic change, the stratigraphy, fossil taxa, and paleoenvironment of these units are the focus of this study.

1.3. Geologic and depositional context

The Cajon Pass lies at the junction of the San Bernardino and San Gabriel Mountains of the Transverse Ranges, where the Crowder Formation and Cajon Valley Formation (formerly known as the Miocene Punchbowl Formation of Woodburne and Golz, 1972) represent separate continental basins now physically adjacent due to movement along the Squaw Peak Fault (Fig. 1). At the time of deposition, these basins are estimated to have been separated by tens of kilometers (Meisling and Weldon, 1989). Sediments of both the Crowder and Cajon Valley formations are primarily arkosic sandstones and conglomerates that were deposited unconformably over crystalline basement rocks or the early Miocene Vaqueros Formation, a marine conglomerate and sandstone locally exposed below the Cajon Valley Formation (Noble, 1954; Dibblee, 1967; Woodburne and Golz, 1972; Morton and Miller, 2006). The composite section of the Crowder Formation contains 980 m of terrestrial sandstones and conglomerates alternating with fine-grained sandstone and siltstone beds (Foster, 1980; Winston, 1985). The Cajon Valley Formation is approximately 2440 m thick and primarily composed of siltstone, arkosic sandstone, and conglomerate with greater lithologic variation (e.g., lignite and limestone present) and sediment induration than the Crowder Formation (Woodburne and Golz, 1972; Meisling and Weldon, 1989). Paleoelevations of these formations are not known; however, regional geological history indicates that uplift northwest and northeast of Cajon Pass supplied sediment to the Crowder and Cajon Valley formations, which were deposited on a low-relief surface proximal to the coast prior to the late Miocene uplift of the Transverse Ranges (Meisling and Weldon, 1989; Woodburne, 1991).

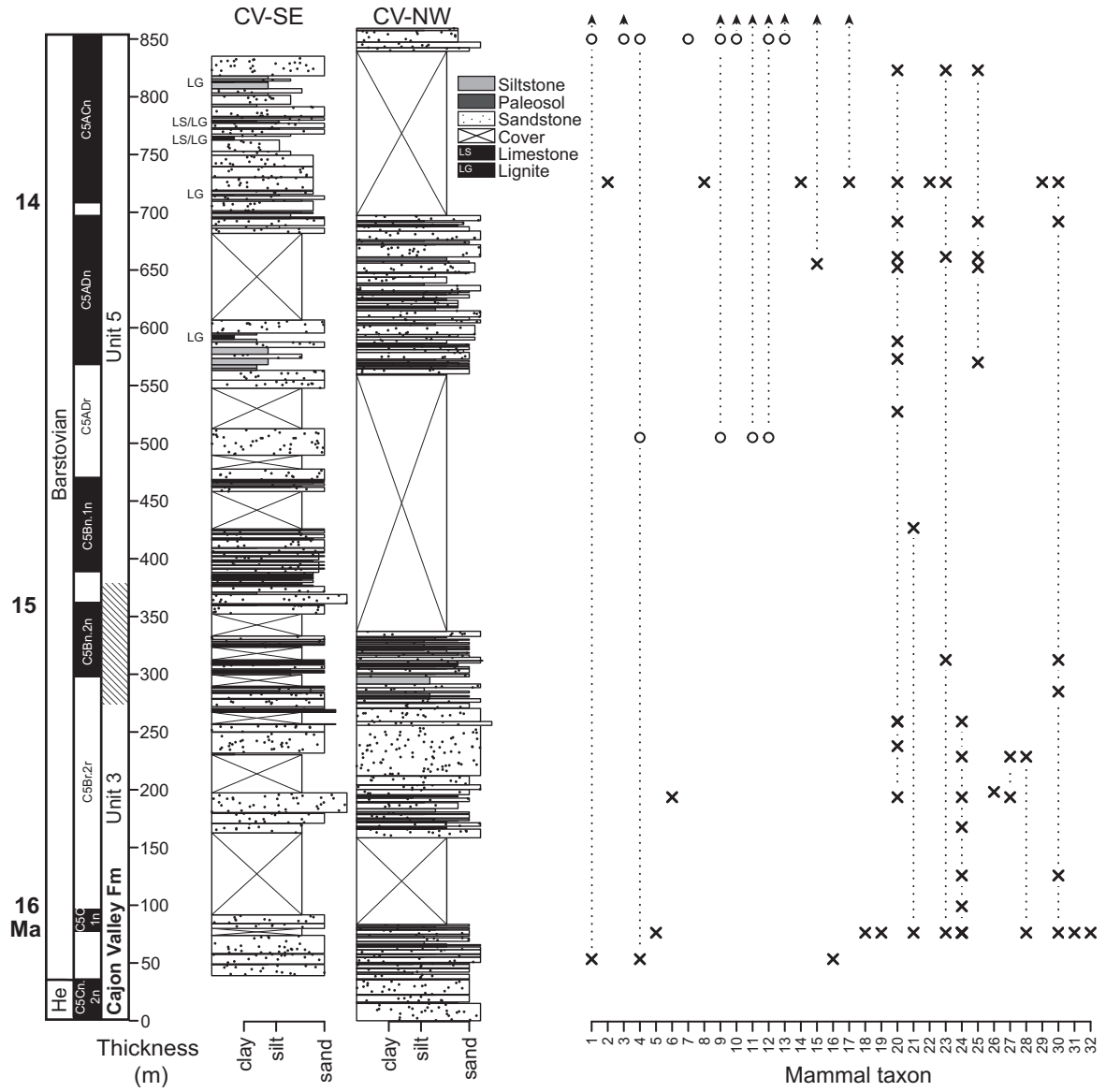

Fig. 3. Southeastern (CV-SE) and northwestern (CV-NW) stratigraphic sections for the Cajon Valley Formation Units 3 and 5 (gradual transition between units indicated by hashed lines). Temporal correlation with the NALMA and global geomagnetic polarity timescales (Woodburne, 1987; Gradstein et al., 2004) is shown. Known (x) and approximate (o) fossil occurrences of taxa (as listed in Table 2) are presented in relation to the stratigraphic section. Biostratigraphic ranges (dotted lines) are assumed to range through the first and last occurrences of taxa within the formation. Arrows indicate fossil occurrences stratigraphically higher than the measured section (Upper Unit 5 and Unit 6). Ages of the sedimentary strata and fossil localities are based on biostratigraphy in Woodburne and Golz (1972) and from paleomagnetic data and age interpretation in Liu (1990).

Based on lithologies, clast composition, sedimentary structures, and bedforms, the depositional environments for the Crowder and Cajon Valley formations are interpreted as fluvial in nature, with features most closely resembling braided channel and floodplain systems in extensional basins (Woodburne and Golz, 1972; Foster, 1980; Winston, 1985; Meisling and Weldon, 1989). Exposures of the Crowder and Cajon Valley formations extend laterally for 35 km and 20 km, respectively, suggesting deposition in broad basins over a low-relief landscape of eroded crystalline bedrock (Noble, 1954; Woodburne and Golz, 1972; Weldon, 1986). For both formations, clast lithologies and cobble imbrication indicate paleocurrent directions with southward and southwestward transport of sediment from terranes in the Mojave Block and Victorville highlands to the north (Woodburne and Golz, 1972; Foster, 1980). Fining-upward lithologies and the presence of lignites and limestone beds in the southeastern portion of the Cajon Valley Formation imply gradual infilling of basins over a southwest-draining paleoslope (Foster, 1980; Weldon, 1986; Meisling and Weldon, 1989). In the Crowder and Cajon Valley formations, mammal fossils are typically associated with finer-grained sandstone and siltstone beds that often contain clays, evidence of root traces, and other pedogenic features (Winston, 1985; Reynolds, 1991).

1.4. Paleoenvironmental reconstructions

Lignites and preserved *Celtis* seeds present in Unit 5 of the Cajon Valley Formation provide an indication of wet, forested habitats during the Barstovian (Woodburne and Golz, 1972; Reynolds, 1991). However, additional records of paleovegetation, including fossil leaves, pollen, phytoliths, or preserved soil organic matter, were otherwise previously unknown from the Cajon Valley and Crowder formations. Phytoliths are silica bodies formed within and between the cells of vascular plants and are readily incorporated into soils during plant decay (e.g., Piperno, 1988). Phytoliths have high preservation potential, especially in paleosols, which are often devoid of plant macrofossils and palynomorphs (Strömberg, 2004), and have been the basis for recognizing major vegetation shifts in the past, such as the regional expansion of North

American grassland ecosystems through the Cenozoic (Strömberg, 2002, 2004, 2006; Edwards et al., 2010; Strömberg and McInerney, 2011). A subset of phytoliths with distinct morphologies are useful for identifying plants at various taxonomic levels and distinguishing among woody vegetation (e.g., forest), C_3-grass, and C_4-grass indicator taxa (Strömberg, 2004; Piperno, 2006; Strömberg and McInerney, 2011). Bulliform phytoliths, other non-diagnostic grass morphotypes, and diatoms found in paleosol samples can additionally produce useful information about the paleo-humidity of the local environment (Bremond et al., 2005).

The relative abundance of C_3 and C_4 vegetation in an ecosystem can be independently recorded by the stable carbon isotope composition of preserved soil organic matter, expressed as $\delta^{13}C_{SOM}$ (e.g., Koch, 1998). In terrestrial settings, photosynthetic pathway is the dominant control on vegetation $\delta^{13}C$ values, with C_3 plants strongly discriminating against ^{13}C during CO_2 fixation relative to C_4 plants (e.g., Smith and Epstein, 1971), which results in distinct, non-overlapping carbon isotope compositions for these groups (Cerling et al., 1997). Enrichment factors relative to atmospheric CO_2 are generally $-19.6‰$ for C_3 vegetation and $-4.7‰$ for C_4 vegetation (Passey et al., 2002), and implementation of linear-mixing models using these values can lead to useful estimates of C_4 vegetation on the landscape. However, fractionation factors are not always constant through time or across space and have been shown to vary as a function of vegetation type, phylogenetic grouping, and past atmospheric CO_2 and O_2 concentrations (Lomax et al., 2012; Porter et al., 2017). In addition, variation around the mean carbon isotope composition of C_3 vegetation ($\delta^{13}C_{C3}$) is related to aridity, with decreased fractionation of atmospheric CO_2 during photosynthesis under water stress (e.g., Farquhar et al., 1989; Passey et al., 2002). This physiological response results in a significant negative relationship between foliar carbon isotope composition and mean annual precipitation, as documented for modern C_3 plants across diverse biomes (Diefendorf et al., 2010; Kohn, 2010). Thus, variation in $\delta^{13}C_{SOM}$ derived from plant material, such as leaf litter (von Fischer and Tieszen, 1995), can be used to infer relative changes in plant water stress and local aridity within ancient pure-C_3 ecosystems (e.g., Freeman et al., 2011).

Quantitative paleoprecipitation (mean annual precipitation or MAP) estimates can be derived from the elemental geochemistry of paleosols, providing an independent measure of water availability in ancient ecosystems. For example, the chemical index of alternation minus potassium (*CIA-K*) serves as a measure of rock or soil weathering (Maynard, 1992), and is calculated by taking the molar ratio of alumina (Al_2O_3) to alumina, lime (CaO), and soda (Na_2O) and multiplying it by 100. *CIA-K* has an observed strong positive relationship to MAP in modern soils (Sheldon et al., 2002), and is therefore a useful proxy for estimating MAP in paleosols. This approach for estimating paleoprecipitation has been applied broadly to Miocene and older paleosols (e.g., Retallack, 2007; Hyland et al., 2013a), and compares well to independent estimation methods (e.g., Wilf et al., 1998; Hyland and Sheldon, 2016). Together, phytolith assemblages, $\delta^{13}C_{SOM}$ data, and *CIA-K* estimates can differentiate ecosystem shifts due to changing C_4 vegetation and/or moisture conditions.

2. Materials and methods

2.1. Field methods

In the Crowder Formation, we measured four sections over 0.5 km and traced beds through covered intervals to produce one continuous composite section (Fig. 2). The composite stratigraphic section was ~110 m thick and spanned upper Unit 1 and Unit 2 of the Crowder Formation east of Interstate 15 in Cajon Pass (Fig. 1). In the Cajon Valley Formation, we measured northwestern (CV-NW) and southeastern (CV-SE) sections (~850 m each; Fig. 3) from exposures of Units 3 and 5 along railroad cuts west of Interstate 15 and north and south of Highway 138. Unit 4 occurs discontinuously or may be a lateral facies of the more widespread Unit 5 elsewhere in the formation (Woodburne and Golz, 1972) and was not present in either of the measured sections. The Cajon Valley sections are approximately three kilometers apart, although at least one fault, the Cleghorn Fault associated with the San Andreas Fault System, separates them (Morton and Miller, 2006). Both sections were measured continuously (including through covered sections where railroad cuts did not expose the underlying rock), and the northwestern and southeastern sections were correlated by the base of Unit 3 and the transition between Units 3 and 5 (Fig. 3). We selected the locations of the sections to incorporate as many previously sampled San Bernardino County Museum and University of California-Riverside fossil localities as possible and to align with sections sampled in earlier paleomagnetic studies (Woodburne and Golz, 1972; Winston, 1985; Weldon, 1986; Liu, 1990; Reynolds et al., 2008). Our measured sections either followed the measured paleomagnetic section (i.e., CV-NW, Crowder Unit 1) or were correlated on the basis of unit boundaries and the stratigraphic distribution of sampled siltstone horizons (i.e., CV-SE, Crowder Unit 2). Unit thicknesses and boundaries in measured sections are similar to the sections from which paleomagnetic data were collected, thereby enabling age inference of stratigraphic units, rock samples, and fossil localities.

We collected samples for bulk soil organic matter (SOM), phytoliths, and elemental geochemistry analyses from the finer-grained siltstone beds exhibiting features of paleosol development (e.g., high clay content, slickensides, root traces, carbonate development). Because the tops of paleosols typically preserve the most phytoliths (Strömberg, 2002) and SOM can become enriched in ^{13}C at depth due to microbial decomposition (Wynn et al., 2005), we collected fresh samples from the uppermost paleosol horizons with the highest concentration of root traces when present. We collected 28 paleosol samples from the Crowder section, every 4.5 m on average and ranging from 0.3 to 27.0 m apart depending on paleosol distribution and degree of development. From the CV-SE and CV-NW sections, we collected 34 and 42 paleosol samples, respectively. The sampling interval varied in relation to the distribution of paleosols and was on average every 23.0 m for CV-SE and 11.0 m for CV-NW. From these field samples, we selected a subset of paleosols for further laboratory analysis ($n = 53$) based on clay content, presence of visible SOM, absence of contaminants (e.g., modern roots), and association with fossil-bearing horizons.

2.2. Laboratory methods

We processed paleosol samples from the measured units of the Crowder and Cajon Valley formations for phytolith extraction ($n = 24$) according to the methodology of Strömberg et al. (2007). Following disaggregation by dissolution in 10% HCl, 1–2 g of homogenized sample material was sieved at two different mesh sizes, 250 μm and 53 μm, and cleaned of organic matter using a concentrated solution of HNO_3 and $KClO_3$. We then separated the biosilica fraction of the sample via $ZnBr_2$ heavy-liquid floatation (specific gravity of 2.38) and mounted the extracts on immersion oil (Cargille Type A) and mounted (Cargille Meltmount 1.539) slides. Slides were analyzed and photographed using a Leica petrographic microscope at a range of magnifications (400–1000 ×). For samples yielding countable assemblages (> 200 diagnostic phytoliths, $n = 18$), we categorized phytoliths by plant functional group based on morphotypes documented in modern reference collections of Strömberg (2003, 2004, 2005). Forest Indicators (FI), which are commonly produced by trees and woody vegetation, included compound variables FI-GEN, DICOT, and PALM, while Grass Indicators (GI), which are grass silica short cells commonly produced by C_3 and C_4 grasses, comprised compound variables GRASS (mainly C_3), POOID (C_3), and PACMAD clade (C_3/C_4), including PANI (panicoid grasses, mainly C_4) and CHLOR (C_4 chloridoid grasses). Other non-diagnostic morphotypes (OTH), those with unclear affinities or known environmental biases (GRASS-ND; Strömberg, 2003, 2011; McInerney

et al., 2011), and non-plant biosilica (e.g., diatoms), were excluded from counts related to calculating FI and GI proportions. Photographs of phytolith and other non-diagnostic morphotypes are in the Supplementary Data (Supplementary Fig. 1). We calculated confidence intervals for each counted sample using a bootstrapping script in R (R Core Development Team, 2013), following procedures of Strömberg (2009) and Chen et al. (2015).

For carbon isotope analysis of organic matter, we selected and cleaned bulk paleosol samples ($n = 53$) in methanol to remove modern carbon and in dilute (7%) HCl to dissolve carbonates (e.g., Cotton et al., 2012). We then crushed samples to homogenize them and weighed them into tin capsules. We analyzed samples for weight percent carbon and $\delta^{13}C_{SOM}$ using a Costech elemental analyzer attached to a Finnigan Delta V+ isotope ratio mass spectrometer at the Stable Isotope Laboratory at the University of Michigan. Results are reported in units per mil relative to Vienna Pee Dee Belemnite (VPDB). International Atomic Energy Agency (IAEA) sucrose and caffeine standards were used to normalize measured values to VPDB, with a standard analytical error of < 0.1‰. We conducted replicate analyses for > 25% of the samples, resulting in an average sample standard error of ~0.5‰.

We analyzed clay-rich samples from the preserved B-horizons of weakly-developed Alfisols found in the Crowder ($n = 1$) and CV-SE ($n = 3$) sections for major elemental composition via X-ray fluorescence (XRF). XRF analyses of whole-rock samples were conducted at the ALS Chemex Lab in Vancouver, BC, Canada, with an average analytical uncertainty of 0.001% and a replicate standard deviation of 0.1%.

2.3. Quantitative inference for paleoenvironmental reconstruction

Based on countable phytolith assemblages from the Crowder ($n = 8$), CV-SE ($n = 5$), and CV-NW ($n = 5$) sections and morphotype identification following Strömberg (2003, 2004, 2005), we calculated the percentages of forest, C_3-grass, and potential C_4-grass indicators as a fraction of the total diagnostic morphotypes. Potential C_4-grass indicators include diagnostic grass silica short cells (GSSCs) from the chloridoid, panicoid and other PACMAD subgroups. Chloridoids and panicoids are predominantly C_4 groups today, while other PACMAD phytoliths belong to either C_3 or C_4 grasses (Strömberg, 2005). Therefore, the total PACMAD (chloridoid + panicoid + PACMAD) phytolith count presented herein represents a maximum C_4 estimate (Strömberg and McInerney, 2011). Representational biases have been documented in modern phytolith assemblages compared to aboveground biomass and may lead to the overestimation of grass indicators within an ecosystem (Strömberg, 2004; Hyland et al., 2013b). However, this bias is minor in Inceptisols (1.7%), which is the predominant paleosol type in the Cajon Valley and Crowder formations, and is generally less than phytolith counting error for the paleosols examined here. Therefore, it was not necessary to apply correction factors to the phytolith counts, and we interpreted the relative proportion of grass phytoliths in these paleosol samples as the relative abundance within the local environment. We additionally tallied the total number of bulliforms and other non-diagnostic grass morphotypes, which have been linked to evapotranspiration (Bremond et al., 2005), and diatoms from each assemblage as an independent moisture-related index.

To compare paleosol $\delta^{13}C_{SOM}$ with the carbon isotope composition of C_3 and C_4 vegetation during the middle Miocene, we adjusted the isotopic composition of end-member C_3 and C_4 values according to the average $\delta^{13}C$ composition of atmospheric CO_2 for 1-myr time bins through the MCO (e.g., Fox et al., 2012). Based on benthic foraminifera reconstructions from Tipple et al. (2010; 3-myr moving average values), $\delta^{13}C_{CO2}$ values ranged from −5.9‰ to −5.3‰ during the middle Miocene. We converted the $\delta^{13}C$ value for the C_3 and C_4 endmembers based on shifting atmospheric CO_2 values and isotopic enrichment factors from Passey et al., 2002; for example, mean $\delta^{13}C_{C3}$ ranged from −24.9‰ to −25.5‰ through the sections. We calculated arid-C_3 endmembers per 1-myr interval by increasing mean $\delta^{13}C_{C3}$ values by one standard deviation (+2.3‰) from the Cerling et al. (1997) global plant isotopic dataset. This offset is comparable to that used in previous studies (+2.9‰) between average C_3 and drought-stressed C_3 endmember values (Passey et al., 2002; Fox et al., 2012). The cut-off value of $\delta^{13}C_{SOM}$ from pure-C_3 vegetation was assumed to be two standard deviations above the $\delta^{13}C_{C3}$ endmember, or approximately −20.5‰, depending on shifting $\delta^{13}C_{CO2}$ values. To test for trends in phytolith and $\delta^{13}C_{SOM}$ data in relation to stratigraphic position (as a measurement of relative geologic age) we applied a Spearman's correlation test to the datasets. Differences in phytolith and isotopic composition between the Crowder and Cajon Valley formations and sections were assessed using a Welch's *t*-test statistic to account for unequal variance between samples.

We calculated the *CIA-K* proxy using the elemental geochemistry of the B-horizon from a subset of our paleosol samples for which the proxy is applicable ($n = 4$). This proxy cannot be used for paleosols without a B-horizon, paleosols derived from limestone parent rock, paleosols on hillslopes or in poorly-drained environments, or on laterites or Vertisols (Sheldon et al., 2002; Nordt and Driese, 2010); therefore, any paleosols exhibiting these features (e.g., paleosols associated with lignites, paleosols lacking B-horizons) were not analyzed. Based on the relationship between *CIA-K* and mean annual precipitation in modern soils, we applied the following transfer function developed by Sheldon et al. (2002) to estimate paleoprecipitation:

$$\text{MAP (mmyr}^{-1}) = 221e^{0.0197(CIA-K)} \quad (\text{SE} = \pm 182 \text{ mmyr}^{-1}\ R^2 = 0.72). \tag{1}$$

2.4. Quantitative inference for faunal assemblages

To compare paleoenvironmental reconstructions with mammalian faunas of the Crowder and Cajon Valley formations, we compiled fossil data from various publications, field reports, and database records from the San Bernardino County Museum (Supplementary Table 1). Because of differences in collection and documentation methods across these resources, data compilation included stratigraphic (and therefore temporal) occurrences of species, but not species abundance data. Specimens were previously identified to taxonomic family and when possible to genus and species based on distinct morphological features, typically of the dentition (Woodburne and Golz, 1972; Reynolds, 1991; Pagnac, 2006; Reynolds et al., 2008). We additionally assigned dietary categories from taxon-specific data and references provided by the Paleobiology Database (www.paleobiodb.org; accessed July 2017) and classified each mammal taxon as either small bodied (typically < 1 kg, mostly includes rodent and lagomorph taxa) or large bodied (e.g., Equidae, Antilocapridae, Rhinocerotidae). Major dietary categories include generalized herbivores, granivores (seed-eating), browsers, and browser-grazers, suggesting mixed dietary sources.

We assigned species biostratigraphic ranges within each formation based on the stratigraphic position of fossil localities where they were found and assuming species ranged through gaps in fossil preservation. A lack of reliable abundance data and different levels of taxonomic resolution inhibit rarefaction analyses in order to estimate species richness in a robust manner (e.g., Raup, 1975; Foote, 1992); therefore, variation in species richness through time may result from differences in preservation and/or sampling. However, the number of species present through time may also reflect real losses and gains in local species richness or compositional turnover, especially for the systematically sampled and screen-washed Crowder Formation. While we were unable to apply sample-size standardization approaches to explicitly test for changes in species richness, we did assign confidence intervals to the stratigraphic ranges of individual taxa following methods and calculations outlined in Marshall (1990). Because observed stratigraphic ranges almost always underestimate true taxonomic longevity, 50% confidence intervals were assigned for the top,

bottom, or both of a taxon's range based on the duration of the observed temporal range of occurrence data and the number of horizons documented for each taxon. These approaches help ensure that uncertainty in first and last appearance occurrences does not dramatically influence potential interpretations of faunal turnover or loss.

We assessed faunal dissimilarity and spatial turnover in species composition between the two formations by counting the number of unique taxa within the Crowder and Cajon faunal assemblages. To determine if the number of unique taxa differed from expected based on random samples (with the same number of taxa as empirical observations) from the combined taxonomic pool for the Crowder and Cajon Valley formations, we performed a bootstrap analysis using a custom script in R (R Core Development Team, 2013). Because identifications differed in taxonomic resolution (e.g., *Petauristodon uphami* is found in the Cajon Valley Formation, while *Petauristodon* sp. is found in the Crowder Formation), we counted a minimum number of shared taxa, assuming unidentified species were always different and a maximum number of shared taxa, assuming they were always equivalent. The number of unique species (either minimum or maximum) was considered significantly different from the null expectation if the observed value fell outside of the 95% bootstrapped confidence interval derived from 1000 random samples.

3. Results

3.1. Stratigraphic framework

The composite section through Units 1 and 2 of the Crowder Formation is approximately 110 m thick and spans the Hemingfordian to Barstovian transition (Fig. 2). Unit 1 of the Crowder Formation (17.0–15.5 Ma) is primarily composed of massive and poorly sorted medium to coarse arkosic sandstone with conglomeratic lenses of heterogeneous subrounded to subangular clasts. Sandstone beds vary in thickness (range: 0.2–26.0 m), are typically < 3.5 m thick (median = 1.6 m), and persist laterally for several hundred meters. Conglomeratic lenses are 3.0–6.0 m across and up to 1.0 m thick and can exhibit graded bedding, cobble imbrication, and planar and trough cross-bedding. Laterally extensive tabular beds of laminated siltstone and fine sandstone with notable clay content are a distinct feature of upper Unit 1. The tops of these thin beds are generally altered by pedogenesis, and when paleosols could be identified to soil order, features most closely matched those of Inceptisols or occasional weak Alfisols. We interpret sandstone beds with channel macroform deposits (e.g., bars and dunes) as a series of active, low-sinuosity streams (Collinson, 1978; Foster, 1980; Winston, 1985). The contact between Units 1 and 2 is gradual (estimated ~15.5 Ma), with Unit 2 composed primarily of arkosic wacke with a higher content of fine sandstone, sandy siltstone, and claystone than Unit 1. Thick fine-grained beds are laterally persistent with lenses of more indurated coarse sandstone and well-rounded pebbles, as well as small-scale, cut-and-fill structures and gravel-stringer deposits. These sandstone lenses represent channel deposits incised into the lower fine-grained floodplain deposits. Sand is dispersed throughout the silty-claystones, including within lenticular clay-rich units that display red and green mottling and other pedogenic features. The transition from the sandstone-dominated Unit 1 to the silt and claystone-dominated Unit 2 represents the transition from a sandy braided-river system to a lower gradient meandering floodplain system with more interchannel sediments preserved (Collinson, 1978; Foster, 1980; Winston, 1985). Paleosols throughout upper Unit 1 and Unit 2 represent surfaces exposed between flooding events and are the primary source of mammal fossils recovered from the Crowder Formation. Fossils collected by previous researchers (see references in Supplementary Table 1) were found in situ as isolated teeth, broken mandibles, or unarticulated limb elements during paleontological surveys (mostly large mammals) and through large-scale screen washing and sorting of matrix during road excavations (large and small mammals).

In contrast, roughly contemporaneous Units 3 and 5 of the Cajon Valley Formation represent significantly more lithological variation over space and through time (Fig. 3). Unit 3 contains several sequences of well-indurated, light-colored coarse sandstones and conglomerates alternating with less resistant, reddish-brown, finer-grained sandstones and siltstones that often preserve pedogenic features. Within the measured sections, Unit 5 overlies Unit 3 and contains a sequence of heterogeneous beds. Unit 5 in the southeastern section includes mottled maroon, gray, and yellow coarse sandstones and conglomerates, green siltstones, and black mudstones with localized plant-bearing lignite beds and freshwater limestones. Unit 5 in the northwestern section is lithologically similar, but lacks the mudstone, lignite, and limestone beds (Woodburne and Golz, 1972).

Approximately 850 m of sediment were deposited in the Cajon Valley Formation from ~16.5–13.7 Ma, indicating a higher rate of sediment accumulation than for the Crowder Formation. In the CV-SE and CV-NW sections, the dominant sandstone beds range in thickness from 0.2 to 43.5 m, and most beds are < 4 m thick (median = 1.8 m). Tabular sandstone beds can display large-scale (up to several meters) trough cross-bedding, imbricated cobbles, and basal scouring. The tops of sandstone beds typically exhibit weak pedogenic horizons and are noted for distinct color changes (red or mottled purple and green), greater clay content, and prominent post-depositional features, such as drab-haloed root traces. The transition from Unit 3 to Unit 5 (~15.0 Ma) represents a gradual increase in the frequency of sandstone and red paleosol alternations. Unit 5 is composed of heterogeneous strata with notable color variation, but few red paleosol horizons. Units 3 and 5 comprise many tabular channel units and are consistent with a bed-load dominated, braided-stream system with periodic soil development (Collinson, 1978). The presence of freshwater limestones and lignites containing plant debris and diatoms in the southeastern section indicate spatial variation in depositional environments across the basin, with localized pond development in the topographic low of the basin center, compared to continuous active-channel deposits in the more marginal northwestern portion of the basin (e.g., Woodburne and Golz, 1972; Foster, 1980). Fossils from the Cajon Valley Formation were collected by previous researchers (see Supplementary Table 1) primarily from paleosol beds and a green silty-sandstone bed adjacent to lignite and freshwater limestone deposits in Unit 5 of CV-SE. Collection methods included ground surveys for in situ material and large-scale matrix removal for screen washing and sorting of large and small vertebrate fossils. Similar to the Crowder Formation, fossils are mostly unarticulated, with isolated teeth or mandible fragments comprising the bulk of identifiable material.

3.2. Vegetation composition and paleoprecipitation

Not all processed paleosol samples produced phytoliths or adequate sample sizes (> 200 diagnostic phytoliths) for counting. Samples vary in preservation quality (e.g., several phytoliths exhibited surficial etching or breakage; see Supplementary Tables 2A–C) and frequently contain morphotypes that were not diagnostic of a specific plant group (Supplementary Fig. 1). The coarser Cajon Valley paleosols (CV-SE and CV-NW) have fewer productive samples than the Crowder paleosols; however, all three sections produced records comprising several different phytolith morphotypes.

3.2.1. Crowder Formation

Phytolith assemblages (n = 8) of the Crowder Formation yielded 17 morphotypes that include forest, C_3-grass, and potential C_4-grass indicators (Fig. 4A; Supplementary Table 2A). Phytoliths from C_4 grasses contribute minimally to the overall vegetation composition, ranging from 7% (95% CI = 4–10%) to 12% (95% CI = 7–16%) of the total phytolith composition. These results provide the earliest potential record of C_4 grasses in the Mojave Region at approximately 17 Ma. However, it should be noted that minimum C_4 estimates show low (3%)

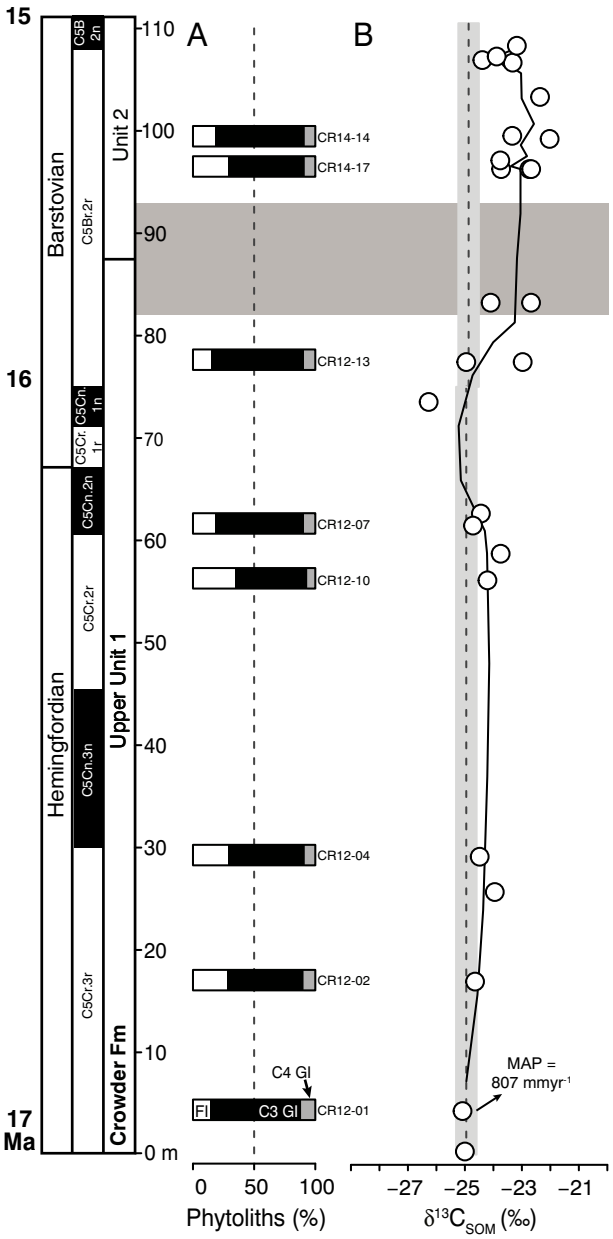

Fig. 4. Paleoenvironmental reconstruction of the Crowder Formation during the MCO. A. Vegetation estimates based on phytolith assemblages: % C_3-forest (white), C_3-grass (black), and C_4-grass (gray) morphotypes. CV# refers to sample ID listed in Supplementary Table 2A. B. Carbon isotope composition of preserved soil organic matter (SOM) with mean C_3 isotopic composition under shifting average $\delta^{13}C_{CO2}$ values (black dashed line), with 90% confidence intervals (gray bars) from Tipple et al. (2010). The trend line is a 3-point moving average. MAP estimate based on *CIA-K* elemental chemistry is given where measured. The horizontal gray bar indicates the interval of most pronounced environmental and faunal change. FI = Forest indicators; GI = Grass indicators.

to no C_4 vegetation since PACMAD, PANI, and CHLOR compound morphotypes often indicate, but are not strictly from C_4 grasses. The phytolith assemblages contain a substantially higher proportion of grass morphotypes, ranging from 65% (95% CI = 59–72%) to 86% (95% CI = 81–91%), than forest morphotypes, ranging from 14% (95% CI = 9–19%) to 35% (95% CI = 28–41%). There is no significant change in forest or grass composition ($r = 0.08$, $p = 0.84$) or in the potential contribution of C_4 grasses ($r = -0.35$, $p = 0.40$) through the section. Diagnostic forest indicators are predominantly from a single 'general' forest indicator morphotype (small rugulose sub-spheres, CI-7), but also include two dicot morphotypes and a palm morphotype. The majority of grasses comprise open-habitat C_3-grass indicators and include four distinct pooid morphotypes, with generic conical rondels (CO-1) dominating the record. Potential C_4-grass morphotypes include one PACMAD, one chloridoid, and two panicoid morphotypes. The total number of bulliforms and other non-diagnostic grass indicator morphotypes (GRASS-ND) plus diatoms (humidity index, or HUM, in Supplementary Table 2A) ranges from 29 to 58 and does not vary significantly through the section ($r = -0.48$, $p = 0.23$).

The $\delta^{13}C_{SOM}$ values for the Crowder Formation range from −26.3‰ to −22.0‰ (Fig. 4B; Supplementary Table 3). With enriched $\delta^{13}C_{CO2}$ values during the MCO (Tipple et al., 2010) and a corresponding 'cut-off' value of approximately −20.5‰ for C_3 vegetation, these values are consistent with predominately C_3 vegetation throughout the section. Because there is no significant change in the relative C_4 phytolith abundance through the section, we cannot attribute major changes in $\delta^{13}C_{SOM}$ to an increased presence of C_4 grasses on the local landscape. A significant positive trend in $\delta^{13}C_{SOM}$ ($r = 0.68$, $p < 0.01$) may instead represent changes in plant water stress and therefore local moisture conditions. The most striking shift in $\delta^{13}C_{SOM}$ occurs during the Barstovian (at 75-85 m in Fig. 4B), without a corresponding change in phytolith composition, indicating drying in the basin through the MCO. Prior to this shift, *CIA-K* estimated MAP was 807 (± 182) mm yr^{-1}, implying a relatively wet ecosystem at ~17.0 Ma (Fig. 4B; Supplementary Table 4).

3.2.2. Cajon Valley Formation

Phytolith samples from the southeastern section of the Cajon Valley Formation (CV-SE; $n = 5$) record a mixture of forest and C_3-grass indicator types (Fig. 5A; Supplementary Table 2B). The proportion of forest indicator types ranges from to 31% (95% CI = 25–37%) to 44% (95% CI = 36–50%), while the proportion of C_3-grass indicators ranges from 56% (95% CI = 50–64%) to 68% (95% CI = 62–74%). The relative phytolith composition does not change significantly through time ($r = 0.30$, $p = 0.68$). Evidence for C_4 grasses is minimal (maximum estimate = 2%); however, these percentages are within counting error (± 1–2%) of zero. Phytolith assemblages from this section comprise four forest indicator morphotypes (Cl-7 and Cl-4 are most common) and four C_3-grass morphotypes, of which two pooids (KR-1 and CO-1) dominate the assemblages (Supplementary Table 2B). The total number of humid-linked morphotypes and diatoms ranges from 47 to 73, with the highest value found in the lignite-associated sample, and does not vary significantly through the section ($r = 0.70$, $p = 0.23$). The carbon isotope composition of this section indicates a pure-C_3 environment, with $\delta^{13}C_{SOM}$ ranging from −28.0‰ to −23.7‰ (Fig. 5B, Supplementary Table 3). These values are both lower and more variable than the carbon isotope composition of soil organic matter from the Crowder Formation, consistent with the potential absence of C_4 vegetation, wetter conditions (i.e., lignites and freshwater limestones present), and greater lithological variation. There is no significant trend in $\delta^{13}C_{SOM}$ through the section ($r = 0.20$, $p = 0.44$). The *CIA-K* index for three late Hemingfordian Alfisol/Inceptisols supports an average MAP estimate of 765 (± 182) mm yr^{-1} for the southeastern part of the basin at ~16–15 Ma (Fig. 5B; Supplementary Table 4).

Phytolith assemblages from the northwestern section of the Cajon Valley Formation (CV-NW; $n = 5$) similarly record a greater proportion of grass indicators than forest indicators (Fig. 5A). The proportion of forest indicator types ranges from to 30% (95% CI = 23–36%) to 42% (95% CI = 35–47%), while the proportion of C_3-grass indicators ranges from 56% (95% CI = 51–63%) to 69% (95% CI = 63–76%). Similar to the CV-NW section, no significant change in relative phytolith composition is found through time ($r = 0.10$, $p = 0.95$). Phytoliths from potential C_4 grasses are low or absent, ranging from 0% to 2% (95% CI = 0–5%). Four forest and four C_3-grass morphotypes are present throughout the section, with Cl-4 and Cl-7 as the most common forest morphotypes (Supplementary Table 2C). Pooids, and in particular one pooid morphotype (generic conical rondel, CO-1), dominate these

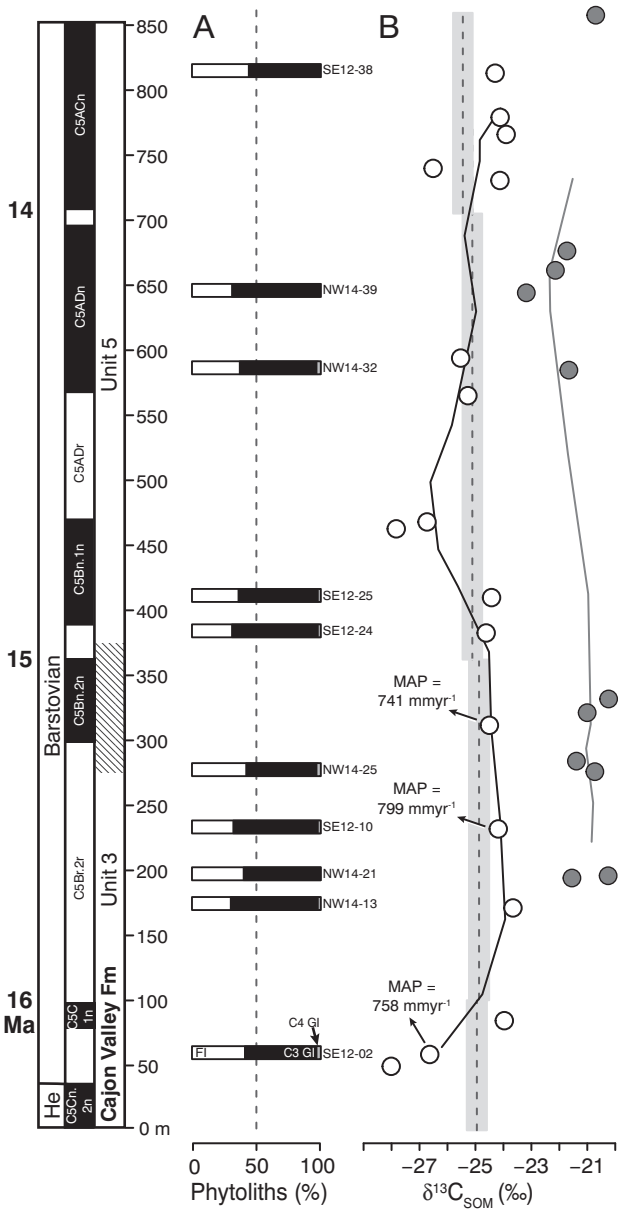

Fig. 5. Paleoenvironmental reconstructions of the southeastern (CV-SE) and northwestern (CV-NW) sections of the Cajon Valley Formation during the MCO. A. Vegetation estimates based on phytolith assemblages: % C_3-forest (white), C_3-grass (black), and C_4 grass (gray) morphotypes. SE# and NW# refer to sample ID listed in Supplementary Tables 2B and 2C. B. Carbon isotope composition of preserved soil organic matter (SOM) with mean C_3 isotopic composition under shifting average $\delta^{13}C_{CO2}$ values (black dashed line), with 90% confidence intervals (gray bars) from Tipple et al. (2010). A 3-point moving-average trend line runs through the CV-SE (white circles) and CV-NW (gray circles) data. MAP estimates based on *CIA-K* elemental chemistry (CV-SE only) are given where measured. FI = Forest indicators; GI = Grass indicators.

assemblages. The total number of humid-linked morphotypes and diatoms ranges from 48 to 69 and does not vary significantly through the section ($r = 0.90$, $p = 0.08$). The $\delta^{13}C_{SOM}$ values range from −23.2‰ to −20.2‰ with no significant trend through time ($r = -0.35$, $p = 0.29$) and do not overlap with values from the southeastern section (Fig. 5B; Supplementary Table 3). Assuming either a mean C_3-endmember value of approximately −25.1‰ or arid C_3-endmember value assumption of approximately −22.8‰ (e.g., see endmember calculation in Methods 2.3), enriched CV-NW $\delta^{13}C_{SOM}$ values indicate some C_4 vegetation was likely present in the northwest section of the Cajon Valley Formation.

3.2.3. Intra- and inter-basin comparison

There is no significant difference in the relative abundance of forest and grass indicators between the Cajon Valley CV-SE and CV-NW sections ($p = 0.73$). In contrast, there is a significant difference in $\delta^{13}C_{SOM}$ values ($p \ll 0.001$) between the two sections, with higher values in the CV-NW section. The relative abundance of grass and forest phytoliths differs significantly between the Crowder and Cajon Valley formations ($p < 0.01$), and the $\delta^{13}C_{SOM}$ values from the Crowder Formation differ from the CV-SE ($p < 0.01$) and CV-NW ($p \ll 0.01$) sections. The Crowder Formation phytolith assemblages record a greater abundance of C_3 grasses and potential C_4 grasses than do phytolith assemblages from the Cajon Valley Formation, while $\delta^{13}C_{SOM}$ values fall between those recorded by the isotopically distinct Cajon Valley sections. The total number of humid-linked morphotypes and diatoms is significantly different between the Crowder and Cajon Valley formation phytolith assemblages ($p = 0.01$); however, it does not differ significantly between the two Cajon Valley sections ($p = 0.60$; see Supplementary Fig. 2).

3.3. Mammalian faunal assemblages

3.3.1. Crowder Formation

The mammal faunas of the Crowder Formation consist of 32 taxa, 21 of which are small-mammals, including 15 rodent species, several lagomorph (rabbits, hares, and pikas) species, an insectivorous shrew-relative, and two mustelid species (Table 1). Of the 11 large mammal taxa, seven are browsers (e.g., several camelid species) and three are considered to be mixed feeders or 'grazer-browsers' (e.g., the equid *Parapliohippus carrizoensis*). Both small and large mammals are preserved throughout the section, and several individual paleosol units within the Crowder Formation record exceptionally diverse assemblages (Fig. 2). For example, 21 species occur in the basal paleosol of the section, including six species of heteromyids (granivorous, burrowing rodents) and four camels. Paleosol horizons (13 in total) in the section were sampled separately during road excavation and screen-washed for small-mammal fossils (approximately 6000 lbs. of matrix per horizon for a total of 167,000 lbs.; Reynolds et al., 2008). Therefore, changes in small-mammal diversity and taxonomic composition among paleosol horizons should not be due primarily to sampling effects (Reynolds, 1991; Reynolds et al., 2008). Notable differences in faunal composition between Units 1 and 2 of the Crowder Formation include an overall reduction in the number of taxa found from 11 to 8 or fewer taxa, a pronounced loss in heteromyid diversity (~75% loss), and the introduction of lagomorph species to local assemblages (Fig. 2). However, the relative proportion of taxa within dietary categories (e.g., browsers vs. mixed feeders) does not change through time, and browsers remain dominant throughout the record. The addition of 50% confidence intervals to observed stratigraphic ranges (Supplementary Fig. 3) does not alter these general findings; however, faunal loss and taxonomic turnover associated with the transition from Unit 1 to Unit 2 appears more gradual when species ranges are extended to account for incompleteness in the fossil record.

3.3.2. Cajon Valley Formation

The mammal faunas of the Cajon Valley Formation consist of 42 taxa, 25 of which are small mammals, including 19 rodent species (Table 2). The faunal composition of the southeastern and northwestern sections of the Cajon Valley Formation is dominated by large mammals, especially in Unit 3 (Fig. 3). Large mammals include several equid taxa, some of which have long biostratigraphic ranges (e.g., *Archeohippus mourningi*), while species such as *Parapliohippus carrizoensis* and

Table 1
Mammalian faunas of the Crowder Formation.

Small mammals		Dietary category[a]
	Heteromyidae	
1	*Perognathus minutus*	Granivore-browser
2	*Paratrogomys whistleri*	Granivore-browser
3	*Mookomys "altifluminus"*	Granivore-browser
4	*Perognathus furlongi*	Granivore-browser
5	*Proheteromys sulculus*	Granivore-browser
6	*Balantiomys crowderensis*	Granivore-browser
7	*Cupidinimus halli*	Granivore-browser
	Sciuridae	
8	*Protospermophilus sp.*	Granivore-frugivore
9	*Tamias sp.*	Granivore-frugivore
10	*Miospermophilus sp.*	Granivore-frugivore
11	*Petauristodon sp.*	Granivore-frugivore
	Zapodidae	
12	*Megasminthus sp.*	Herbivore
13	*Plesiosminthus sp.*	Herbivore
	Cricetidae	
14	*Copemys tenuis*	Herbivore
15	*Copemys pagei*	Herbivore
16	Heterosoricidae – *Paradomnina relictus*	Insectivore
17	Leporidae – *Hypolagus sp.*	Grazer-browser
	Ochotonidae	
18	*Russellagus sp.*	Herbivore
19	*Hesperolagomys sp.*	Herbivore
	Mustelidae	
20	*Miomustela sp.*	Carnivore-omnivore
21	*Leptarctus sp.*	Omnivore

Large mammals		Dietary category[a]
22	Antilocapridae – cf. *Merycodus sp.*	Browser-grazer
23	Palaeomerycidae – *Sinclairomeryx sp.*	Browser
	Equidae	
24	*Archaeohippus mourningi*	Browser
25	*Parapliohippus carrizoensis*	Grazer-browser
26	"Merychippus" (large)	Grazer-browser
27	Tayassuidae – *Cynorca sp.*	Herbivore-omnivore
	Camelidae	
28	*Procamelus sp.*	Browser
29	*Michenia agatensis*	Browser
30	*Miolabis tenuis*	Browser
31	*Hesperocamelus sp.*	Browser
32	Rhinocerotidae – *Menoceras sp.*	Browser

[a] Data extracted from the Paleobiology Database.

Table 2
Mammalian faunas of the Cajon Valley Formation.

Small mammals		Dietary category[a]
	Heteromyidae	
1	*Cupidinimus sp.*	Granivore-browser
2	*Harrymys maximus*	Granivore-browser
3	*Perognathus furlongi*	Granivore-browser
4	*Proheteromys sulculus*	Granivore-browser
5	Sciuridae	
6	*Petauristodon,* large sp.	Granivore-frugivore
7	*Petauristodon,* small sp.	Granivore-frugivore
8	*Petauristodon uphami*	Granivore-frugivore
	Cricetidae	
9	*Copemys longidens*	Herbivore
10	*Copemys* sp. cf. *C. russelli*	Herbivore
11	*Copemys tenuis*	Herbivore
	Eomyidae	
12	*Pseudadjidaumo stirtoni*	Herbivore
	Geomyidae	
13	*Mojavemys lophatus*	Browser
14	Heterosoricidae – *Paradomnina relictus*	Insectivore
15	Talpidae	Insectivore
16	Leporidae – *Hypolagus sp.*	Grazer-browser
17	Erinaceidae – *Lanthanotherium sp.*	Insectivore-carnivore
18	Mustelidae – *Leptarctus ancipidens*	Omnivore

Large mammals		Dietary category[a]
19	Antilocapridae	Browser-grazer
20	Camelidae	Browser
21	Chalicotheriidae – *Moropus sp.*	Browser
	Equidae	
22	*Acritohippus stylodontus*	Grazer-browser
23	*Archaeohippus mourningi*	Browser
24	*Parapliohippus carrizoensis*	Grazer-browser
25	*Scaphohippus intermontanus*	Grazer-browser
26	Merycoidodontidae – *Brachycrus buwaldi*	Herbivore
27	Moschidae – Blastomerycine	Browser-grazer
	Palaeomerycidae	
28	*Bouromeryx americanus*	Browser
29	*Bouromeryx sp.*	Browser
30	Rhinocerotidae	Browser
31	Tayassuidae – *Dyseohyus sp.*	Herbivore-omnivore
32	Ursidae – *Ursavus sp.*	Herbivore-carnivore

Unit 6 taxa: *Cupidinimus halli* (granivore-herbivore), *C. lindsayi* (granivore-herbivore), *Miospermophilus* (granivore-frugivore), *Spermophilus* sp. cf. *S. primitivus* (granivore-frugivore), *Mojavemys alexandrae* (browser), *Parapliosaccomys* (browser), *Hypolagus fontinalis* (grazer-browser).
Unit 5, above stratigraphic section: *Aepycamelus alexandrae* (browser), *Dyseohyus fricki* (herbivore-omnivore), *Scaphohippus sumani* (grazer-browser).

[a] Data extracted from the Paleobiology Database.

Scaphohippus intermontanus are restricted to Units 3 and 5, respectively. Small-mammal taxa are less common throughout the Cajon Valley Formation, perhaps due to differences in sampling effort and other taphonomic processes. For example, screen-washing efforts within the formation were less systematic than those carried out in the Crowder Formation, making relative changes in the number of species through the stratigraphic section difficult to interpret. However, small mammals do contribute to the increased taxonomic richness found in two highly-productive localities (at ~70 m and ~730 m) and in the younger Unit 6 of the Cajon Valley Formation (Fig. 3). The addition of 50% confidence intervals to the observed stratigraphic ranges adds little resolution to trends in species richness through time (Supplementary Fig. 4), and apart from three cricetid taxa with poorly-known occurrences, the stratigraphic ranges of most taxa remain restricted to Unit 3, Unit 5, or span the entire record as shown in Fig. 3. Most species are characterized as browsers (Table 2), and there is no noticeable shift in the relative proportion of browsing taxa through the record.

3.3.3. Inter-basin comparison

Faunal assemblages from each basin comprise a greater number of unique taxa than shared taxa. For the Crowder Formation, 22–44% of the total mammalian fauna is shared with the Cajon Valley Formation, assuming minimum and maximum number of shared taxa (see description in Methods 2.4). For the Crowder assemblages, 24–43% of small-bodied taxa are shared with Cajon Valley assemblages compared to 18–45% of shared large-bodied taxa. For the Cajon Valley Formation, 32–40% of mammalian taxa are shared with the Crowder Formation. Small-bodied taxa are more commonly shared (28–48%) than large-bodied taxa (12–30%). Based on random resampling of the combined taxonomic pool, the number of shared taxa (minimum or maximum

Table 3
Results from bootstrap analysis of faunal similarity.

Minimum shared	Bootstrapped distribution[a]	Observed value	
	Mean (95% CI)	Crowder	Cajon Valley
Total taxa	21 (17–25)	7	9
Small-mammal taxa	14 (10–17)	5	7
Large-mammal taxa	7 (5–10)	2	2

Maximum shared	Bootstrapped distribution[a]	Observed value	
	Mean (95% CI)	Crowder	Cajon Valley
Total taxa	24 (21–27)	14	17
Small-mammal taxa	16 (13–18)	9	12
Large-mammal taxa	8 (6–10)	5	5

[a] The number of unique taxa expected under null expectations according to the bootstrapped distribution of faunal similarity values.

estimate) is always below the lower bound of the 95% confidence interval generated from the bootstrapping approach (Table 3).

4. Discussion

4.1. Spatio-temporal variation in paleovegetation

The Crowder and Cajon Valley formations provide a record of paleoenvironment, vegetation distribution, and faunal assemblages during a major global warming interval. Independent evidence from phytolith assemblages and carbon isotope composition of soil organic matter indicate primarily C_3 ecosystems within the Crowder and Cajon Valley formations, with spatial variability in the relative abundance of grasses, and in particular potential C_4-grasses, recorded within the three sections. The consistently low presence of PACMAD, including panicoid and chloridoid phytoliths, in the Crowder Formation provides the earliest potential evidence of C_4 grasses in the Mojave region. Phytoliths from C_4 grasses may also be present through the Cajon Valley Formation, but if present (relative proportion is within counting error of zero), C_4 vegetation and grass phytoliths are significantly less abundant in the Cajon Valley Formation than in the Crowder Formation. Although the *CIA-K* index does not suggest major differences in moisture conditions between the two basins, the humidity-index (total number of bulliforms and other non-diagnostic grass morphotypes plus diatoms, e.g., Bremond et al., 2005) is significantly different between the two basins, with a lower abundance of humidity-linked indicators in the Crowder Formation (Supplementary Fig. 2). These differences between the two basins suggest habitat heterogeneity at the scale of 10s of kilometers during the Miocene.

Within the Cajon Valley basin, predominantly C_3-phytolith assemblages do not differ significantly between two measured sections separated by ~3 km. However, spatial variation in $\delta^{13}C_{SOM}$ indicate that local relief, moisture conditions, and habitat heterogeneity influenced the degree of water stress experienced by above-ground vegetation across the basin. Enriched values of $\delta^{13}C_{SOM}$ in the CV-NW section may be recording a water-stressed C_3 ecosystem within a more arid or well-drained region of the basin. Lower $\delta^{13}C_{SOM}$ values in the CV-SE section support the interpretation of a poorly-drained and occasionally wet depositional environment independently inferred from lignites and limestone deposits found in the section. Vegetation structure, and in particular canopy density, can influence $\delta^{13}C_{SOM}$ through mechanisms related to soil moisture as well, with enriched $\delta^{13}C_{SOM}$ values correlated with increased ecosystem openness and aridity (Ladd et al., 2014). However, lateral variation in vegetation structure and leaf area index has yet to be explored with these phytolith data (e.g., Dunn et al., 2015). Together, alternating active channel deposits and weakly-developed paleosol horizons, phytolith assemblage with > 50% C_3-grasses, and enriched $\delta^{13}C_{SOM}$ in the CV-NW section likely represent a grassland ecosystem, potentially with a small amount of C_4 grass, in a well-drained environment along the basin margin. In contrast, the CV-SE section represents a C_3 ecosystem that became poorly drained as the basin filled with sediment, eventually leading to shallow freshwater and swamp deposits near the basin depocenter after ~14 Ma.

Alternative explanations for differences in $\delta^{13}C_{SOM}$ values throughout the depositional history of the Crowder and Cajon Valley basins include varying C_4 grass abundance that was not preserved in the phytolith record. This seems unlikely given the similar degree of phytolith preservation among the three sections. Changing $\delta^{13}C_{SOM}$ values could also be related to shifts in plant functional type or phylogenetic affinity and associated variation in CO_2 fractionation from the atmosphere (Lomax et al., 2012; Porter et al., 2017); however, the phytolith record does not show turnover in dominant morphotypes and thus plant groups through time. Changing CO_2 and O_2 concentrations may additionally influence plant fractionation values and the $\delta^{13}C_{SOM}$ record. Since middle Miocene atmospheric conditions are still an area of active research (e.g., Beerling and Royer, 2011; Goldner et al., 2014), this remains a difficult explanation to assess for the Crowder and Cajon Valley formations. Differences in $\delta^{13}C_{SOM}$ values across space could also be exaggerated or attenuated due to differences in soil respiration and carbon turnover rates, with enriched isotopic values corresponding with increased soil respiration (e.g., Wynn et al., 2005; but see Breecker et al., 2009). Elevated soil carbon turnover and respiration appear to be related to higher temperatures (Trumore, 2000; Knorr et al., 2005)—like those experienced during the MCO—and increased precipitation and/or soil moisture (Raich and Schlesinger, 1992; Cotton and Sheldon, 2012). These processes could contribute to the positive trend in the Crowder $\delta^{13}C_{SOM}$ record over time or in the spatial variation found between the CV-SE and CV-NW records. However, given predominantly well-drained depositional environments in both basins (most samples are derived from thin paleosols that alternate with active channel deposits) and the continental-scale aridification trend unfolding during the middle to late Miocene, we find the previously proposed explanation to be more likely. Future testing of herbivore tooth enamel could clarify the relative roles of aridity, C_4 vegetation, and other potential drivers determining $\delta^{13}C_{SOM}$ values in the Crowder and Cajon Valley formations (e.g., Kohn, 2010).

The Crowder and Cajon Valley records extend the geographic scope of phytolith assemblage analyses and represent the first combined records of local vegetation and climate from the southwestern Basin and Range Province during the MCO. Although there is little plant macrofossil material and no pollen known from the Crowder and Cajon Valley formations, the vegetation composition inferred from phytoliths can be compared with plant fossil localities of similar age elsewhere in the Mojave Desert, including the Barstow Formation. The Barstow Formation has a sparse plant fossil record that includes fossilized impressions of both forest (palms and woody dicots including potential pine, walnut, hackberry, and juniper species) and grass species (Alf, 1970; Reynolds and Schweich, 2013; Reynolds and Schweich, 2015). The presence of C_4 grasses in the Barstow Formation by 14.3 Ma is documented from the isotopic composition of ungulate tooth enamel, with equids recording up to 18% C_4 dietary composition (Feranec and Pagnac, 2013). Similar analysis of tooth enamel revealed no evidence for the consumption of C_4 vegetation by equids from the Cajon Valley Formation (Feranec and Pagnac, 2017), suggesting that C_4 grasses were an emerging food resource found locally only in the Crowder basin prior to 14.3 Ma. The contemporaneous Tehachapi Flora (15.5–11.8 Ma) on the western edge of the Mojave region was also a mixed woodland, with temperate oaks, conifers, palms, and several sclerophyllous shrub taxa as evidenced by macrofloral fossils (Axelrod, 1939, 1979).

Spatial and temporal variation in vegetation as well as the

asynchronous appearance of C_4 grasses within the Mojave suggests that a mosaic of heterogeneous habitats, including C_3 grasslands, characterized the regional landscape as early as the middle Miocene. These records match paleoenvironmental reconstructions based on phytoliths elsewhere in the intermontane west (Cotton et al., 2012; Chen et al., 2015; Harris et al., 2017) and in the Great Plains (Strömberg, 2004; Strömberg and McInerney, 2011), which indicate mixed grassy and wooded patches throughout the early to middle Miocene and the subsequent spread of grasslands during the late Miocene (Strömberg, 2005; Edwards et al., 2010; Strömberg, 2011). Additional evidence from macrofossils and pollen suggest that the progressive spread of savanna, woodland, and shrubland after the MCO paralleled global cooling and regional aridification (Wolfe, 1985; Leopold and Denton, 1987; Pound et al., 2012; Hyland et al., *in review*). While, the primary driver of the C_4-grass expansion globally remains unresolved, recent studies have documented temporal and regional variation in this expansion and suggest that multiple factors may have led to increasing C_4 grass proportions across ecosystems (Edwards et al., 2010; Fox et al., 2012, Cotton et al., 2014). Spatial heterogeneity of C_4 grasses between the Crowder and Cajon Valley basins supports the hypothesis that expansion of C_4 ecosystems was influenced by local factors instead of global climate and CO_2 drivers (Fox and Koch, 2003; Edwards et al., 2010; Strömberg and McInerney, 2011; Cotton et al., 2012; Chen et al., 2015; Hyland et al., *in review*). Integration of phytolith and $\delta^{13}C_{SOM}$ data provides a multi-proxy reconstruction of the middle Miocene Mojave vegetation, and facilitates the distinction between open, closed, and mixed C_3-dominated ecosystems and between water-stressed C_3 vegetation and low-abundance C_4 plants on the landscape.

4.2. Terrestrial paleoclimate reconstructions for the MCO

Terrestrial temperature records during the MCO indicate that mean annual temperatures were 6.8 ± 2.2 °C warmer than today on average, although there is considerable variation in paleotemperature estimates depending on geographic location and the temperature proxy used (Pound et al., 2012; Goldner et al., 2014). The oxygen and hydrogen isotope composition of smectites from the Barstow Formation between 15.8 and 14.8 Ma yield mean annual temperature estimates of 26 °C, or ~8 °C warmer than mean annual temperatures in the region today (Mix and Chamberlain, 2014). Paleoprecipitation estimates of 807 (± 182) and 765 (± 182) mm yr^{-1} from the Crowder and Cajon Valley formations during this warm interval agree with other regional records (Wolfe, 1985; Sheldon, 2006; Pound et al., 2012). Based on the composition of fossil-plant assemblages, Basin and Range Province precipitation ranged from 381 to 635 mm yr^{-1} in temperate xerophytic shrubland (Axelrod, 1939) and from 760 to 890 mm yr^{-1} in mixed-forest ecosystems (Axelrod, 1995). MAP estimates derived from the elemental geochemistry (*CIA-K*) of paleosols from the Picture Gorge Basalts of central Oregon (USA) decreased from 900 to 500 mm yr^{-1} during the second half of the MCO, indicating Miocene aridification in the northern Basin and Range (Sheldon, 2006).

Given global and regional climate trends during the MCO, relatively little change in phytolith assemblages or the carbon isotope composition of preserved SOM recorded over the depositional histories of the Crowder and Cajon Valley basins is a surprising finding. The main exception is a significant positive shift in $\delta^{13}C_{SOM}$ values from 17 to 15 Ma in the Crowder Formation without a corresponding increase in C_4-grass phytolith abundance, implying a drying trend within the predominantly C_3 ecosystem. The apparent stability of local environmental conditions and vegetation composition during the MCO global warming interval may be explained by climate moderation due to the coastal proximity of these basins on the former landscape (e.g., Vallis, 2011). Because the deposition of the Crowder and Cajon Valley formations occurred prior to the late Miocene to early Pliocene uplift of the Transverse Ranges (Meisling and Weldon, 1989), the absence of topographic barriers between the Pacific Ocean and these basins would have reduced orographic climate effects and could have dampened continental climate fluctuations experienced by more inland basins. Higher relative abundance of grasses and lower counts of humidity-related indicators in the Crowder Formation may be attributed to its position further inland (Meisling and Weldon, 1989).

4.3. Environmental significance for mammalian faunas

Linking paleoenvironmental reconstructions with changes in taxonomic richness and composition of mammalian faunas requires dense and well-resolved records for fossil assemblages, vegetation, and paleoclimate. In the Crowder Formation, 21 small-mammal species occur continuously in at least 13 stratigraphic levels, suggesting a diverse faunal composition through the Hemingfordian to early Barstovian interval of the MCO (~17–15.7 Ma; Table 1). The most prominent change in species composition and decline in taxonomic richness in the Crowder Formation involved the loss of heteromyid (pocket mouse) taxonomic dominance and the first appearance of three lagomorph species at ~16 Ma (Fig. 2). This faunal change coincided with a notable change from predominantly braided-stream deposits with intermittent and weakly-developed paleosols (upper Unit 1) to more frequent and well-developed paleosols in a floodplain-dominated system (Unit 2). While changes in depositional environment, and thus taphonomic processes, through time can influence the number of specimens and species preserved, floodplain systems are generally thought to have better preservation potential than braided-stream systems (e.g., Koster, 1987; Behrensmeyer, 1988). Therefore, taxonomic turnover and species loss is not explained by the transition in depositional environment alone. Bone breakage patterns can also inform the degree of taphonomic overprinting on faunal assemblages. While the Crowder small-mammal record is mainly composed of isolated teeth, more complete mandible fragments are also found above and below this transition (Reynolds et al., 2008; Lindsay and Reynolds, 2015), suggesting taphonomic filters are similar through the record. Furthermore, the restriction of fossils to paleosol beds suggests that similar environments were recorded through time, which were then sampled with equal effort throughout the record (Reynolds, 1991; Reynolds et al., 2008). We cannot rule out taphonomic processes entirely or apply sample-standardization approaches to this record due to the lack of reliable abundance data; however, taphonomy seems unlikely to be the sole explanatory factor behind the loss of local species richness recorded in the Crowder Formation during the MCO.

The faunal turnover and inferred change in the depositional environment at ~16 Ma also correspond with a significant shift in the carbon isotope record (Fig. 4). Phytolith assemblages through the Crowder Formation consistently record a mixed forest-grassland ecosystem with a low percentage of C_4 vegetation, indicating that the carbon isotope enrichment at this time was influenced by changes in climate and/or water availability rather than a shift in C_4 grass abundance. Although greater support is needed to test the hypothesis (e.g., from additional basins showing similar trends), mammalian faunal turnover and decline in the Crowder basin could be linked to increasing aridity and a corresponding reduction of preferred dietary resources (e.g., more edible vegetation) or total plant biomass during the MCO. Notably, taxonomic turnover does not correspond with an ecological turnover, with browser-dominated faunas occurring both before and after 16 Ma. These results are consistent with the temporal mismatch between early grassland expansion and the later rise of hypsodont and grazer-dominated faunas found in several other Miocene records (Janis et al., 2004; Strömberg, 2006, 2011; Jardine et al., 2012; Strömberg et al., 2013).

In contrast to the Crowder Formation, changes in taxonomic richness in the Cajon Valley Formation are likely controlled by differences in fossil preservation and sampling. Two species-rich localities near the base of Unit 3 and top of Unit 5 are the only departures from otherwise even species richness through time and are the source of most small-

mammal taxa (Fig. 3). Despite this taphonomic bias, small-mammal assemblages differ between Unit 3 (early Barstovian) and Unit 5 (late Barstovian), most notably due to the introduction of cricetids, gophers, insectivores, and lagomorphs to the latter half of the record. With the loss of Palaeomerycidae and Chalicotheriidae taxa and the addition of a Barstovian-aged horse, *Scaphohippus intermontanus*, differences in large-mammal composition also suggest a turnover in faunal composition through the MCO. Paleoenvironmental reconstructions based on the phytolith and $\delta^{13}C_{SOM}$ records from the Cajon Valley Formation indicate a wet climate and relatively open (57–71% grass) vegetation throughout the depositional history of the basin (Fig. 5). Large- and small-mammal faunas contained taxa inferred to be mixed feeders that included browse and grass in their diets (e.g., equids, including *Acritohippus stylodontus*), browsers (e.g., chalicothere, *Moropus*) and small granivores (e.g., heteromyid rodents; Korth, 1994; Janis et al., 2005). The relative number of browsers (high) and grazers (low) does not change through the record. A braided-stream system crossing a broad alluvial plain generated through tectonic extension (e.g., Foster, 1980; Weldon, 1986) and spatial heterogeneity in vegetation and moisture conditions could have supported the observed high local diversity in the Cajon Valley basin.

4.4. Regional mammal diversity and faunal composition

The Crowder and Cajon Valley formations document faunal and vegetation composition during the MCO, including the Hemingfordian interval that is rare elsewhere in western North America, and contribute to our understanding of biological responses to changes in the global climate and local landscape (Barnosky and Carrasco, 2002; Barnosky et al., 2007; Finarelli and Badgley, 2010). This record from the Mojave region provides evidence that elevated regional diversity during the MCO was composed of both high local diversity and high spatial turnover in diversity. Diverse rodent assemblages (up to 10 co-occurring species) characterize the Crowder Formation and include seven species of ecologically-similar heteromyid rodents and six sciurid genera. Similarity, small-mammal taxa of the Cajon Valley Formation are from several rodent families, including heteromyids, sciurids, cricetids, eomyids, and geomyids (Reynolds, 1991; Lindsay and Reynolds, 2008; Reynolds et al., 2008). The Cajon Valley Formation fossil assemblages also contain a diverse large-mammal fauna, including four equid genera, the chalicothere *Moropus*, the oreodont *Brachycrus*, palaeomerycids such as *Bouromeryx*, and tayassuids such as *Dyseohyus* (Woodburne and Golz, 1972; Pagnac, 2006; Coombs and Reynolds, 2015). Taxonomic similarity is low between the two formations (~20–40% shared taxa) despite temporal overlap (inferred ages indicate overlap from ~16.5 to 15.0 Ma), suggesting spatial variation in faunal composition over tens of kilometers. The proportion of unique combined, large, and small mammal species within each formation is far lower (1.5 to 3.5 times lower) than expected based on random subsampling of the regional species pool (Table 3).

Not only do the Crowder and Cajon Valley fossil records differ from one another, contributing to high inter-basin diversity, but they also differ from contemporaneous records elsewhere in the Mojave region. These formations overlap temporally with the Upper Hector Formation in the Cady Mountains and the Barstow Formation within the Mud Hills and vicinity, both of which represent more inland depositional environments separated by topographic barriers today and during the middle Miocene (Woodburne et al., 1974; Meisling and Weldon, 1989; Woodburne et al., 1990). The Hector Formation spans late Arikareean to late Hemingfordian NALMAs from ~22.9–16.0 Ma (Woodburne et al., 1974; Woodburne, 1998). The youngest faunal assemblage, the Upper Cady Mountain Fauna, is late Hemingfordian in age, overlapping with the time represented in the Crowder and Cajon Valley formations (Woodburne, 1991). This fauna has only ~8 species, composed of taxa shared with the Crowder and Cajon Valley Hemingfordian assemblages, such as *Proheteromys sulculus*, *Parapliohippus carrizoensis*, cf. *Merycodus* and Rhinocerotidae (Miller, 1980; Woodburne, 1998). However, several taxa are found in the Hector Formation but not in the Crowder or Cajon Valley formations, including the beaver cf. *Anchitheriomys* and the canid *Tomarctus*. Sampling issues may influence differences found between the Hemingfordian fossil record of the Cady Mountains and that of the Cajon Pass. However, recovery of mammals of similar body size and environmental affinity in both regions supports the concept of high geographic turnover in taxonomic composition at broader spatial scales within the Mojave Region.

Faunas of the Barstow Formation contemporaneous with faunas of the Crowder and Cajon Valley formations are younger than the Upper Cady Mountain Fauna and include the Red Division (16.7 Ma), Rak Division (16.7–16.0 Ma), Green Hills (16.0–15.3 Ma), Second Division (15.3–14.8 Ma), and lower First Division (14.8–13.4 Ma) faunas (Lindsay, 1972; Woodburne et al., 1990; Pagnac, 2009). Differences in small-mammal composition among these formations are especially striking. The late Hemingfordian Red Division faunal assemblage lacks a small-mammal record (despite screen-washing attempts); however, the otherwise diverse small-mammal faunas of the Barstow Formation and Crowder Formation have a greater number of unique genera and species than they do shared species (Lindsay, 1972; Lindsay, 1995). Although small-mammal faunas of the Cajon Valley Formation are less diverse, they also contain species not found in the Barstow Formation, including the large-bodied heteromyid, *Harrymys maximus* (Lindsay and Reynolds, 2015). Large-mammal faunas are more similar than small-mammal faunas across the three formations, suggesting lower spatial turnover for large mammals than for small mammals in the region, as occurs today. However, the Barstow Formation has a notably (~2–3 times, depending on the approximate ages being compared) more diverse large-mammal record, including several canid, oreodont, amphicyonid, and artiodactyl species not found in the Crowder and Cajon Valley formations (Woodburne et al., 1990; Wang et al., 1999; Pagnac, 2009). High spatial turnover and several unique species across this region aligns with previous observations that the MCO was an interval of high zoogeographic provinciality in western North America as interactions between climate change and tectonic activity intensified biogeographic and macroevolutionary processes (Tedford et al., 2004; Badgley and Finarelli, 2013).

5. Conclusions

The middle Miocene was a significant interval of local to regional landscape and climate change, including tectonic extension and the development of topographic complexity in western North America and the MCO warming period, that coincided with peak mammal diversity for the entire Great Basin. The Crowder and Cajon Valley formations provide new paleoenvironmental and faunal information, most notably during the initial MCO warming for which records are currently sparse in western North America. At least 56 mammalian taxa have been collected from these formations, and three sections document changes in depositional environments through time. The integration of phytolith, carbon isotope composition of preserved soil organic matter, and paleosol-derived precipitation proxies provide a detailed reconstruction of spatially and temporally varying paleoenvironmental conditions. These formations record mesic (MAP = ~800 mm yr^{-1}) ecosystems, the development of increasingly arid conditions, the existence of relatively open grassland ecosystems, and the earliest potential evidence of C_4 grasses within the Mojave Desert region and more broadly across the Basin and Range Province.

The Mojave Desert has the longest, most continuous record of mammalian diversity in the Great Basin, and the Crowder and Cajon Valley formations document distinct depositional environments and faunal assemblages compared to the nearby Barstow Formation. Mammalian response to environmental change is evident in the Crowder Formation, which records faunal turnover and declining diversity of small mammals in relation to a drying trend in the basin. Low

faunal similarity between the Crowder, Cajon Valley, and Barstow formations imply high spatial turnover in species composition, while diverse assemblages, especially of small mammals, in the Crowder and Barstow formations and certain paleosol units of the Cajon Valley Formation indicate high local diversity. Both contributed to increased regional diversity and document the history of mammalian diversity during past warming and landscape change.

Acknowledgments

We are grateful for the financial support of this research provided by the Society of Vertebrate Paleontology's Patterson Field Research Award and the University of Michigan's Turner Research Program. We thank Catherine Badgley for field guidance and helpful review of this manuscript, Katharine Loughney, Molly Moroz, Michael Woodburne, Lora Wingate, Tim Gallagher, and Symone Bawol for support in the field and in the laboratory, and Caroline Strömberg for guidance with phytolith identification. We benefitted from comments provided by Isabel Montañez, Robert Feranec, Regan Dunn, and one anonymous reviewer of this manuscript. We thank Eric Scott and the San Bernardino County Museum for access to museum database records, as well as William Sapp and the San Bernardino National Forest Service for providing field permits to make this work possible.

Appendix A. Supplementary data

Supplementary data to this article can be found online at https://doi.org/10.1016/j.palaeo.2017.11.020.

References

Alf, R.M., 1970. A preliminary report on a Miocene flora from the Barstow formation, Barstow, California. Bull. South. Calif. Acad. Sci. 69, 183–189.
Axelrod, D.I., 1939. Miocene flora from the western border of the Mohave Desert. Carnegie Inst. Wash. Publ. 516 (129pp.).
Axelrod, D.I., 1979. Age and origin of Sonoran Desert vegetation. In: Occasional Papers of the California Academy of Sciences. 132 (74pp.).
Axelrod, D.I., 1995. The Miocene Purple Mountain Flora of western Nevada. Geol. Sci. Univ. Calif. Publ. 139, 1–63.
Badgley, C., Finarelli, J.A., 2013. Diversity dynamics of mammals in relation to tectonic and climatic history: comparison of three Neogene records from North America. Paleobiology 39, 373–399.
Badgley, C., Smiley, T.M., Finarelli, J.A., 2014. Great Basin mammal diversity in relation to landscape history. J. Mammal. 95, 1090–1106.
Barnosky, A.D., Carrasco, M.A., 2002. Effects of Oligo-Miocene global climate changes on mammalian species richness in the northwestern quarter of the USA. Evol. Ecol. Res. 4, 811–841.
Barnosky, A.D., Bibi, F., Hopkins, S.S.B., Nichols, R., 2007. Biostratigraphy and magnetostratigraphy of the mid-Miocene railroad canyon sequence, Montana and Idaho, and age of the mid-tertiary unconformity west of the continental divide. J. Vertebr. Paleontol. 27, 204–224.
Beerling, D.J., Royer, D.L., 2011. Convergent Cenozoic CO_2 history. Nat. Geosci. 4, 418–420.
Behrensmeyer, A.K., 1988. Vertebrate preservation in fluvial channels. Palaeogeogr. Palaeoclimatol. Palaeoecol. 63, 183–199.
Breecker, D.O., Sharp, Z.D., McFadden, L.D., 2009. Seasonal bias in the formation and stable isotopic composition of pedogenic carbonate in modern soils from central New Mexico, USA. Geol. Soc. Am. Bull. 121, 630–640.
Bremond, L., Alexandre, A., Peyron, O., Guiot, J., 2005. Grass water stress estimated from phytoliths in West Africa. J. Biogeogr. 40, 311–327.
Cerling, T.E., Harris, J.M., MacFadden, B.J., Leakey, M.G., Quade, J., Eisenmann, V., Ehleringer, J.R., 1997. Global vegetation change through the Miocene/Pliocene boundary. Nature 389, 153–158.
Chen, S.T., Smith, S.Y., Sheldon, N.D., Strömberg, C.A.E., 2015. Regional-scale variability in the spread of grasslands in the late Miocene. Palaeogeogr. Palaeoclimatol. Palaeoecol. 437, 42–52.
Collinson, J.D., 1978. Alluvial Sediments. In: Reading, H.G. (Ed.), Sedimentary Environments and Facies. Blackwell Scientific Publications, Oxford, England, pp. 37–82.
Coombs, M.C., Reynolds, R.E., 2015. Chalicothere material (Perissodactyla, Chalicotheriidae, Schizotherinnae) from late Hemingfordian and early Barstovian faunas of the Cajon Valley Formation in the Mojave Desert Province of southern California. In: Mojave Miocene, Desert Symposium Field Guide and Proceedings, pp. 119–129.
Cotton, J.M., Sheldon, N.D., 2012. New constraints on using paleosols to reconstruct atmospheric pCO_2. Geol. Soc. Am. Bull. 124, 1411–1423.
Cotton, J.M., Sheldon, N.D., Strömberg, C.A.E., 2012. High-resolution isotopic record of C_4 photosynthesis in a Miocene grassland. Palaeogeogr. Palaeoclimatol. Palaeoecol. 337-338, 88–98.
Cotton, J.M., Hyland, E.G., Sheldon, N.D., 2014. Multi-proxy evidence for tectonic control on the expansion of C_4 grasses in northwest Argentina. Earth Planet. Sci. Lett. 395, 41–50.
Dibblee, T.W., 1967. Areal geology of the western Mojave Desert, California. US Geol. Surv. Prof. Pap. 522 (153 pp).
Dickinson, W.R., 2006. Geotectonic evolution of the Great Basin. Geosphere 2, 353–368.
Diefendorf, A.F., Mueller, K.E., Wing, S.L., Koch, P.L., Freeman, K.H., 2010. Global patterns in leaf ^{13}C discrimination and implications for studies of past and future climate. Proc. Natl. Acad. Sci. U. S. A. 107, 5738–5743.
Dunn, R.E., Strömberg, C.A.E., Madden, R.H., Kohn, M.J., Carlini, A.A., 2015. Linked canopy, climate, and faunal change in the Cenozoic of Patagonia. Science 347, 258–261.
Edwards, E.J., Osborne, C.P., Strömberg, C.A.E., Smith, S.A., C_4 Grasses Consortium, Bond, W.J., Christin, P.A., Cousins, A.B., Duvall, M.R., Fox, D.L., Freckleton, R.P., Ghannoum, O., Hartwell, J., Huang, Y., Janis, C.M., Keeley, J.E., Kellogg, E.A., Knapp, A.K., Leakey, A.D.B., Nelson, D.M., Saarela, J.M., Sage, R.F., Sala, O.E., Salamin, N., Still, C.J., Tipple, B., 2010. The origins of C_4 grasslands: integrating evolutionary and ecosystem science. Science 328, 587–591.
Farquhar, G.D., Ehleringer, J.R., Hubick, K.T., 1989. Carbon isotope discrimination and photosynthesis. Annu. Rev. Plant Biol. 40, 503–537.
Feranec, R.S., Pagnac, D., 2013. Stable carbon isotope evidence for the abundance of C_4 plants in the middle Miocene of southern California. Palaeogeogr. Palaeoclimatol. Palaeoecol. 388, 42–47.
Feranec, R.S., Pagnac, D., 2017. Hypsodonty, horses, and the spread of C_4 grasses during the middle Miocene in southern California. Evol. Ecol. Res. 18, 201–223.
Figueirido, B., Janis, C.M., Pérez-Claros, J.A., De Renzi, M., Palmqvist, P., 2012. Cenozoic climate change influences mammalian evolutionary dynamics. Proc. Natl. Acad. Sci. U. S. A. 109 722–272.
Finarelli, J.A., Badgley, C., 2010. Diversity dynamics of Miocene mammals in relation to the history of tectonism and climate. P. R. Soc. B-Biol. Sci. 277, 2721–2726.
Foote, M., 1992. Rarefaction analysis of morphological and taxonomic diversity. Paleobiology 18, 1–16.
Foster, J.F., 1980. Late Cenozoic Tectonic Evolution of Cajon Valley, Southern California (Ph.D. thesis). University of California Riverside (238pp.).
Fox, D.L., Koch, P.L., 2003. Tertiary history of C_4 biomass in the Great Plains, USA. Geology 31, 809–812.
Fox, D.L., Honey, J.G., Martin, R.A., Peláez-Campomanes, P., 2012. Pedogenic carbonate stable isotope record of environmental change during the Neogene in the southern Great Plains, southwest Kansas, USA: carbon isotopes and the evolution of C_4-dominated grasslands. Geol. Soc. Am. Bull. 124, 444–462.
Freeman, K.H., Mueller, K.E., Diefendorf, A.F., Wing, S.L., Koch, P.L., 2011. Clarifying the influence of water availability and plant types on carbon isotope discrimination by C_3 plants. Proc. Natl. Acad. Sci. U. S. A. 108, E59–E60.
Goldner, A., Herold, N., Huber, M., 2014. The challenge of simulating the warmth of the mid-Miocene climatic optimum in CESM1. Clim. Past 10, 523–536.
Gradstein, F.M., Ogg, J.G., Smith, A.G. (Eds.), 2004. A Geologic Time Scale 2004. Cambridge University Press, New York.
Harris, E.B., Strömberg, C.A.E., Sheldon, N.D., Smith, S.Y., Vilhena, D.A., 2017. Vegetation response during the lead-up to the middle Miocene warming event in the Northern Rocky Mountains, USA. Palaeogeogr. Palaeoclimatol. Palaeoecol. 485, 401–415.
Hyland, E., Sheldon, N.D., 2016. Examining the spatial consistency of palaeosol proxies: implications for palaeoclimatic and palaeoenvironmental reconstructions in terrestrial sedimentary basins. Sedimentology 63, 959–971.
Hyland, E., Sheldon, N.D., Fan, M., 2013a. Terrestrial paleoenvironmental reconstructions indicate transient peak warming during the early Eocene climatic optimum. Geol. Soc. Am. Bull. 125, 1338–1348.
Hyland, E., Smith, S.Y., Sheldon, N.D., 2013b. Representational bias in phytoliths from modern soils of central North America: implications for paleovegetation reconstructions. Palaeogeogr. Palaeoclimatol. Palaeoecol. 374, 338–348.
Hyland, E.G., Sheldon, N.D., Smith, S.Y., Strömberg, C.A.E., 2017. Late Miocene rise and fall of C4 grasses in the western United States linked to aridification and uplift. Earth Planet. Sci. Lett (in review).
Janis, C.M., Damuth, J., Theodor, J.M., 2000. Miocene ungulates and terrestrial primary productivity: where have all the browsers gone? Proc. Natl. Acad. Sci. U. S. A. 97, 7899–7904.
Janis, C.M., Damuth, J., Theodor, J.M., 2004. The species richness of Miocene browsers, and implications for habitat type and primary productivity in the North American grassland biome. Palaeogeogr. Palaeoclimatol. Palaeoecol. 207, 371–398.
Janis, C.M., Scott, K.M., Jacobs, L.L. (Eds.), 2005. Evolution of Tertiary Mammals of North America. Cambridge University Press, Cambridge, United Kingdom.
Jardine, P.E., Janis, C.M., Sahney, S., Benton, M.J., 2012. Grit not grass: concordant patterns of early origin of hypsodonty in Great Plains ungulates and Glires. Palaeogeogr. Palaeoclimatol. Palaeoecol. 365–366, 1–12.
Knorr, W., Prentice, I.C., House, J.I., Holland, E.A., 2005. Long-term sensitivity of soil carbon turnover to warming. Nature 433, 298–301.
Koch, P.L., 1998. Isotopic reconstruction of past continental environments. Annu. Rev. Earth Planet. Sci. 26, 573–613.
Kohn, M.J., 2010. Carbon isotope compositions of terrestrial C_3 plants as indicators of (paleo) ecology and (paleo) climate. Proc. Natl. Acad. Sci. U. S. A. 107, 19691–19695.
Kohn, M.J., Fremd, T.J., 2008. Miocene tectonics and climate forcing of biodiversity, western United States. Geology 36, 783–786.
Korth, W.K., 1994. The Tertiary Record of Rodents in North America. Plenum Press, New

York.
Koster, E.H., 1987. Vertebrate taphonomy applied to the analysis of ancient fluvial systems. In: Ethridge, F.G., Flores, R.M., Harvey, M.D. (Eds.), Recent Development in Fluvial Sedimentology: Society of Economic Paleontologists and Mineralogists, Special Publication 39, pp. 159–168.
Ladd, B., Peri, P.L., Pepper, D.A., Silva, L.C.R., Sheil, D., Bonser, S.P., Laffan, S.W., Amelung, W., Ekblad, A., Eiasson, P., Bahamonde, H., Duarte-Guardia, S., Bird, M., 2014. Carbon isotopic signatures of soil organic matter correlate with leaf area index across woody biomes. J. Ecol. 102, 1606–1611.
Leopold, E.B., Denton, M.F., 1987. Comparative age of grassland and steppe east and west of the northern Rocky Mountains. Ann. Mo. Bot. Gard. 74, 841–867.
Lindsay, E.H., 1972. Small mammal fossils from the Barstow formation, California. Geol. Sci. Univ. Calif. Publ. 93, 1–104.
Lindsay, E.H., 1995. *Copemys* and the Barstovian/Hemingfordian boundary. J. Vertebr. Paleontol. 15, 357–365.
Lindsay, E.H., Reynolds, R.E., 2008. Heteromyid rodents from Miocene faunas of the Mojave Desert, Southern California. In: Wang, X., Barnes, L.G. (Eds.), Geology and Vertebrate Paleontology of Western and Southern North America, Contributions in Honor of David P. Whistler. Science Series 41 Natural History Museum of Los Angeles County, pp. 213–235.
Lindsay, E.H., Reynolds, R.E., 2015. *Harrymys maximus* (James): new interpretation for a Miocene geomyoid rodent. In: Mojave Miocene, Desert Symposium Field Guide and Proceedings, pp. 274–280.
Liu, W., 1990. Paleomagnetism of Miocene Sedimentary Rocks in the Transverse Ranges: The Implications for Tectonic History (Ph.D. thesis). California Institute of Technology (218pp.).
Lomax, B.H., Knight, C.A., Lake, J.A., 2012. An experimental evaluation of the use of C3 δ^{13}C plant tissue as a proxy for the paleoatmospheric δ^{13}CO2 signature of air. Geochem. Geophys. Geosyst. 13, Q0AI03.
Marshall, C.R., 1990. Confidence intervals on stratigraphic ranges. Paleobiology 16, 1–10.
Maynard, J.B., 1992. Chemistry of modern soils as a guide to interpreting Precambrian paleosols. J. Geol. 100, 279–289.
McInerney, F.A., Strömberg, C.A.E., White, J.W.C., 2011. The Neogene transition from C_3 to C_4 grasslands in North America: stable carbon isotope ratios of fossil phytoliths. Paleobiology 37, 23–49.
McQuarrie, N., Wernicke, B.P., 2005. An animated tectonic reconstruction of southwestern North America since 36 Ma. Geosphere 1, 147–172.
Meisling, K.E., Weldon, R.J., 1989. Late Cenozoic tectonics of the northwestern San Bernardino Mountains, southern California. Geol. Soc. Am. Bull. 101, 106–128.
Miller, S.T., 1980. Geology and mammalian biostratigraphy of a part of the northern Cady Mountains, Mojave Desert, California. U.S. Geol. Surv. Open File Rep. 80–878 (127pp.).
Mix, H.T., Chamberlain, C.P., 2014. Stable isotope records of hydrologic change and paleotemperature from smectite in Cenozoic western North America. Geochim. Cosmochim. Acta 141, 532–546.
Morton, D.M., Miller, F.K., 2006. Geologic Map of the San Bernardino and Santa Ana 30′ X 60′ Quadrangles, California. US Geological Survey.
Noble, L.F., 1954. The San Andreas fault zone from Soledad Pass to Cajon Pass, California. In: Geology of Southern California. 170. California Department of Resources, Division of Mines Bulletin, pp. 37–48.
Nordt, L.C., Driese, S.D., 2010. New weathering index improves paleorainfall estimates from Vertisols. Geology 38, 407–410.
Pagnac, D., 2006. *Scaphohippus*, a new genus of horse (Mammalia: Equidae) from the Barstow formation of California. J. Mamm. Evol. 13, 37–61.
Pagnac, D., 2009. Revised large mammal biostratigraphy and biochronology of the Barstow formation (Middle Miocene), California. PaleoBios 29, 48–59.
Passey, B.H., Cerling, T.E., Perkins, M.E., Voorhies, M.R., Harris, J.M., Tucker, S.T., 2002. Environmental change in the Great Plains: an isotopic record from fossil horses. J. Geol. 110, 123–140.
Piperno, D.R., 1988. Phytolith Analysis, an Archaeological and Geological Perspective. Academic Press, San Diego, California.
Piperno, D.R., 2006. Phytoliths: A Comprehensive Guide for Archaeologists and Paleoecologists. AltaMira Press, Lanham, Maryland.
Porter, A.S., Yiotis, C., Montañez, I.P., McElwain, J.C., 2017. Evolutionary differences in Δ^{13}C detected between spore and seed bearing plants following exposure to a range of atmospheric O_2:CO_2 ratios; implications for paleoatmosphere reconstruction. Geochim. Cosmochim. Acta 213, 517–533.
Pound, M.J., Haywood, A.M., Salzmann, U., Riding, J.B., 2012. Global vegetation dynamics and latitudinal temperature gradients during the Mid to Late Miocene (15.97–5.33 Ma). Earth-Sci. Rev. 112, 1–22.
R Development Core Team, 2013. R: A Language and Environment for Statistical Computing. R Foundation for Statistical Computing, Vienna, Austria. www.R-project.org/.
Raich, J.W., Schlesinger, W.H., 1992. The global carbon dioxide flux in soil respiration and its relationship to vegetation and climate. Tellus 44, 81–99.
Raup, D.M., 1975. Taxonomic diversity estimation using rarefaction. Paleobiology 1, 333–342.
Retallack, G.J., 2007. Cenozoic paleoclimate on land in North America. J. Geol. 115, 271–294.
Reynolds, R.E., 1991. Biostratigraphic relationships of tertiary small vertebrates from Cajon Valley, San Bernardino County, California. San Bernardino Cty. Mus. Assoc. Q. 38, 54–59.
Reynolds, R.E., Schweich, T.A., 2013. The Rainbow Loop Flora from the Mud Hills. In: Mojave Desert, California, Desert Symposium Field Guide and Proceedings, pp. 39–48.
Reynolds, R.E., Schweich, T.A., 2015. Additions to the floras of the Barstow Formation in the Mud Hills, Mojave Desert, California. In: Mojave Miocene, Desert Symposium Field Guide and Proceedings, pp. 119–129.
Reynolds, R.E., Reynolds, R.L., Lindsay, E.H., 2008. Biostratigraphy of the Miocene Crowder Formation, Cajon Pass, southwestern Mojave Desert, California. In: Wang, X., Barnes, L.G. (Eds.), Geology and Vertebrate Paleontology of Western and Southern North America, Contributions in Honor of David P. Whistler. Science Series 41 Natural History Museum of Los Angeles County, pp. 237–253.
Riddle, B.R., Jezkova, T., Hornsby, A.D., Matocq, M.D., 2014. Assembling the modern Great Basin mammal biota: insights from molecular biogeography and the fossil record. J. Mammal. 95, 1107–1127.
Samuels, J.X., Hopkins, S.S.B., 2017. The impacts of Cenozoic climate and habitat changes on small mammal diversity of North America. Glob. Planet. Chang. 149, 36–52.
Sheldon, N.D., 2006. Using paleosols of the Picture Gorge basalt to reconstruct the middle Miocene climatic optimum. PaleoBios 26, 27–36.
Sheldon, N.D., Retallack, G.J., Tanaka, S., 2002. Geochemical climofunctions from North American soils and application to paleosols across the Eocene-Oligocene boundary in Oregon. J. Geol. 110, 687–696.
Smith, B.N., Epstein, S., 1971. Two categories of $^{13}C/^{12}C$ ratios for higher plants. Plant Physiol. 47, 380–384.
Strömberg, C.A.E., 2002. The origin and spread of grass-dominated ecosystems in the Late Tertiary of North America: preliminary results concerning the evolution of hypsodonty. Palaeogeogr. Palaeoclimatol. Palaeoecol. 177, 59–75.
Strömberg, C.A.E., 2003. The Origin and Spread of Grass-Dominated Ecosystems during the Tertiary of North America and How It Relates to the Evolution of Hypsodonty in Equids (Ph.D. thesis). Department of Biology, University of California Berkeley (779pp.).
Strömberg, C.A.E., 2004. Using phytolith assemblages to reconstruct the origin and spread of grass-dominated habitats in the great plains of North America during the late Eocene to early Miocene. Palaeogeogr. Palaeoclimatol. Palaeoecol. 207, 239–275.
Strömberg, C.A.E., 2005. Decoupled taxonomic radiation and ecological expansion of open-habitat grasses in the Cenozoic of North America. Proc. Natl. Acad. Sci. U. S. A. 102, 11980–11984.
Strömberg, C.A.E., 2006. Evolution of hypsodonty in equids: testing a hypothesis of adaptation. Paleobiology 32, 236–258.
Strömberg, C.A.E., 2009. Methodological concerns for analysis of phytolith assemblages: does count size matter? Quat. Int. 193, 124–140.
Strömberg, C.A.E., 2011. Evolution of grasses and grassland ecosystems. Annu. Rev. Earth Planet. Sci. 39, 517–544.
Strömberg, C.A.E., McInerney, F.A., 2011. The Neogene transition from C_3 to C_4 grasslands in North America: assemblage analysis of fossil phytoliths. Paleobiology 37, 50–71.
Strömberg, C.A.E., Werdelin, L., Friis, E.M., Saraç, G., 2007. The spread of grass-dominated habitats in Turkey and surrounding areas during the Cenozoic: phytolith evidence. Palaeogeogr. Palaeoclimatol. Palaeoecol. 250, 18–49.
Strömberg, C.A.E., Dunn, R.E., Madden, R.H., Kohn, M.J., Carlini, A.A., 2013. Decoupling the spread of grasslands from the evolution of grazer-type herbivores in South America. Nat. Commun. 4, 1478.
Tedford, R.H., Albright, L.B., Barnosky, A.D., Ferrusquia-Villafranca, I., Hunt, R.M., Storer, J.E., Swisher, C.C., Voorhies, M.R., Webb, S.D., Whistler, D.P., 2004. Mammalian biochronology of the Arikareean through Hemphillian interval (Late Oligocene through Early Pliocene epochs). In: Woodburne, M.O. (Ed.), Late Cretaceous and Cenozoic Mammals of North America: Biostratigraphy and Geochronology. Columbia University Press, New York, pp. 169–231.
Tipple, B.J., Meyers, S.R., Pagani, M., 2010. Carbon isotope ratio of Cenozoic CO_2: a comparative evaluation of available geochemical proxies. Paleoceanography 25, PA3202.
Trumore, S., 2000. Age of soil organic matter and soil respiration: radiocarbon constraints on belowground C dynamics. Ecol. Appl. 10, 399–411.
Vallis, G.K., 2011. Climate and the Oceans. Princeton University Press, Princeton, New Jersey.
von Fischer, J.C., Tieszen, L.L., 1995. Carbon isotope characterization of vegetation and soil organic matter in subtropical forests in Luquillo, Puerto Rico. Biotropica 27, 138–148.
Wang, X., Tedford, R.H., Taylor, B.E., 1999. Phylogenetic systematics of the Borophaginae (Carnivora, Canidae). B. Am. Mus. Nat. Hist. 243, 1–391.
Weldon, R.J., 1986. The Late Cenozoic Geology of Cajon Pass: Implications for Tectonics and Sedimentation along the San Andreas Fault (Ph. D. thesis). California Institute of Technology (400pp.).
Wilf, P., Wing, S.L., Greenwood, D.R., Greenwood, C.L., 1998. Using leaves as paleoprecipitation indicators: an Eocene example. Geology 3, 203–206.
Winston, D.S., 1985. The Physical and Magnetic Stratigraphy of the Miocene Crowder Formation, Cajon Valley Pass, Southern California (Masters thesis). University of Southern California (111pp.).
Wolfe, J.A., 1985. Distribution of major vegetation types during the Tertiary. In: Sundquist, E.T., Broecker, W.S. (Eds.), The Carbon Cycle and Atmospheric CO_2: Natural Variations Archean to Present: Geoph. Monog. 32, pp. 357–377.
Woodburne, M.O. (Ed.), 1987. Cenozoic Mammals of North America: Geochronology and Biostratigraphy. University of California Press, Berkeley, California.
Woodburne, M.O., 1991. The Mojave Desert Province. San Bernardino Cty. Mus. Assoc. Q. 38, 60–77.
Woodburne, M.O., 1998. Arikareean and Hemingfordian faunas of the Cady Mountains, Mojave Desert Province, California. In: Terry Jr.D.O., LaGarry, H.E., Hunt Jr.R.M. (Eds.), Depositional Environments, Lithostratigraphy, and Biostratigraphy of the White River and Arikaree Groups (Late Eocene to Early Miocene, North America):

Boulder, Colorado, Geol. S. Am. S, pp. 197–210.
Woodburne, M.O., Golz, D.J., 1972. Stratigraphy of the Punchbowl Formation, Cajon Valley, Southern California. Geol. Sci. Univ. Calif. Publ. 92, 1–73.
Woodburne, M.O., Tedford, R.H., Stevens, M.S., 1974. Early Miocene mammalian faunas, Mojave Desert, California. J. Paleontol. 48, 6–26.
Woodburne, M.O., Tedford, R.H., Swisher III, C.C., 1990. Lithostratigraphy, biostratigraphy, and geochronology of the Barstow formation, Mojave Desert, southern California. Geol. Soc. Am. Bull. 102, 459–477.
Wynn, J.G., Bird, M.I., Wong, V.N.L., 2005. Rayleigh distillation and the depth profile of $^{13}C/^{12}C$ ratios of soil organic carbon from soils of disparate texture in Iron Range National Park, Far North Queensland, Australia. Geochim. Cosmochim. Acta 69, 1961–1973.
Zachos, J., Pagani, M., Sloan, L., Thomas, E., Billups, K., 2001. Trends, rhythms, and aberrations in global climate 65 Ma to present. Science 292, 686–693.